6. SITE 914[1]

Shipboard Scientific Party[2]

HOLE 914A

Date occupied: 30 September 1993

Date departed: 30 September 1993

Time on hole: 14 hr, 30 min

Position: 63°27.738′N, 39°43.489′W

Bottom felt (drill-pipe measurement from rig floor, m): 544.0

Distance between rig floor and sea level (m): 10.8

Water depth (drill-pipe measurement from sea level, m): 533.2

Total depth (from rig floor, m): 562.60

Penetration (m): 18.6

Number of cores (including cores having no recovery): 4

Total length of cored section (m): 18.60

Total core recovered (m): 11.88

Core recovery (%): 63.9

Oldest sediment cored:
Depth (mbsf): 18.6
Nature: gravel and dropstone
Age: Quaternary
Measured velocity (km/s): 2.1

HOLE 914B

Date occupied: 1 October 1993

Date departed: 3 October 1993

Time on hole: 2 days, 14 hr

Position: 63°27.737′N, 39°43.482′W

Bottom felt (drill-pipe measurement from rig floor, m): 544.0

Distance between rig floor and sea level (m): 10.8

Water depth (drill-pipe measurement from sea level, m): 533.2

Total depth (from rig floor, m): 789.0

Penetration (m): 245.0

Number of cores (including cores having no recovery): 17

Total length of cored section (m): 151.20

Total core recovered (m): 17.78

Core recovery (%): 11.8

Oldest sediment cored:
Depth (mbsf): 245.00
Nature: sandy silt
Age: early Oligocene
Measured velocity (km/s): 2.6

Comments: Washed from 0 to 93.8 mbsf.

HOLE 914C

Date occupied: 3 October 1993

Date departed: 5 October 1993

Time on hole: 1 day, 13 hr, 15 min

Position: 63°27.736′N, 39°43.479′W

Bottom felt (drill-pipe measurement from rig floor, m): 544.0

Distance between rig floor and sea level (m): 10.8

Water depth (drill-pipe measurement from sea level, m): 533.2

Total depth (from rig floor, m): 768.0

Penetration (m): 224.0 m

Number of cores (including cores having no recovery): 0

Core recovery (%): 0

Comments: Drilled from 0 to 224.0 mbsf. No core recovered.

Principal results: Site 914 (proposed Site EG63-1A) is located on the East Greenland Shelf, approximately 60 km from the coast. The site was selected to penetrate a representative sequence of Quaternary and Tertiary sediments commensurate with deep penetration (400 m) of the featheredge of the seaward-dipping reflector sequences (SDRS). The primary objectives at this site were (1) the Quaternary and Holocene glacial histories of the margin; (2) the Paleogene sedimentation and subsidence histories; and (3) the composition, age, and eruption environment of the SDRS.

Originally, we had intended that Site EG63-1 would include a cased, multiple reentry hole for penetrating deep basement. However, a rheologically firm, 120-m-thick layer of glacial diamicton with dropstones led to severe drilling difficulties, and three holes were required. Failure to reach basaltic basement led to our abandoning Site 914 in favor of sites to the west-northwest (Sites 915, 916, and 917), where the basement is at a shallower level.

A summary of the principal drilling results from Site 914 is given in Figure 1. The upper part of the succession cored in Holes 914A and 914B comprises Holocene glaciomarine sandy silt and mud with dropstones (lithologic Subunit IA; 0–5 mbsf), Quaternary compacted diamicton (Subunit IB; 5–14 mbsf), and glaciogenic sediment with gravel clasts, the matrix of which was not recovered (Subunit IC: 14–158.5 mbsf). The interval from 158.5 to 187.2 mbsf was not recovered; however, according to the seismic record, it also is of glaciogenic origin. A 5-cm-thick, ash-bearing layer occurs at interval 152-914A-1H-1, 30–35 cm. The dropstones comprise a variety of lithologic types, including basalt, granite gneiss, and quartzite, and range in size from sand grains to cobbles of at least the width of the core.

Lithologic Unit II (187.2–245.0 mbsf; base not recovered) is characterized by massive, greenish-black sandy silt that has been extensively bioturbated. Detrital grains include quartz, plagioclase, amphiboles, pyroxene, garnet, mica, lithic fragments of basalt, and wood. The presence of a zeolite, phillipsite, indicates alteration of volcanic glass by seawater. Calcareous sandstones occur in Unit II. These contain glauconite and a variety of biogenic detritus, indicating a marine origin for these sediments. Overall, the fine grain size and bioturbation in Unit II suggest a mid- to outer-shelf environment of deposition. The sandy interbeds indicate increased current activity, perhaps related to storms.

Lithologic Unit II has been dated, using calcareous nannofossils, as latest Eocene to early Oligocene age (32–35 Ma). Benthic foraminifers indicate paleowater depths of between 100 and 250 m.

[1] Larsen, H.C., Saunders, A.D., Clift, P.D., et al., 1994. *Proc. ODP, Init. Repts.,* 152: College Station, TX (Ocean Drilling Program).
[2] Shipboard Scientific Party is as given in list of participants preceding the contents.

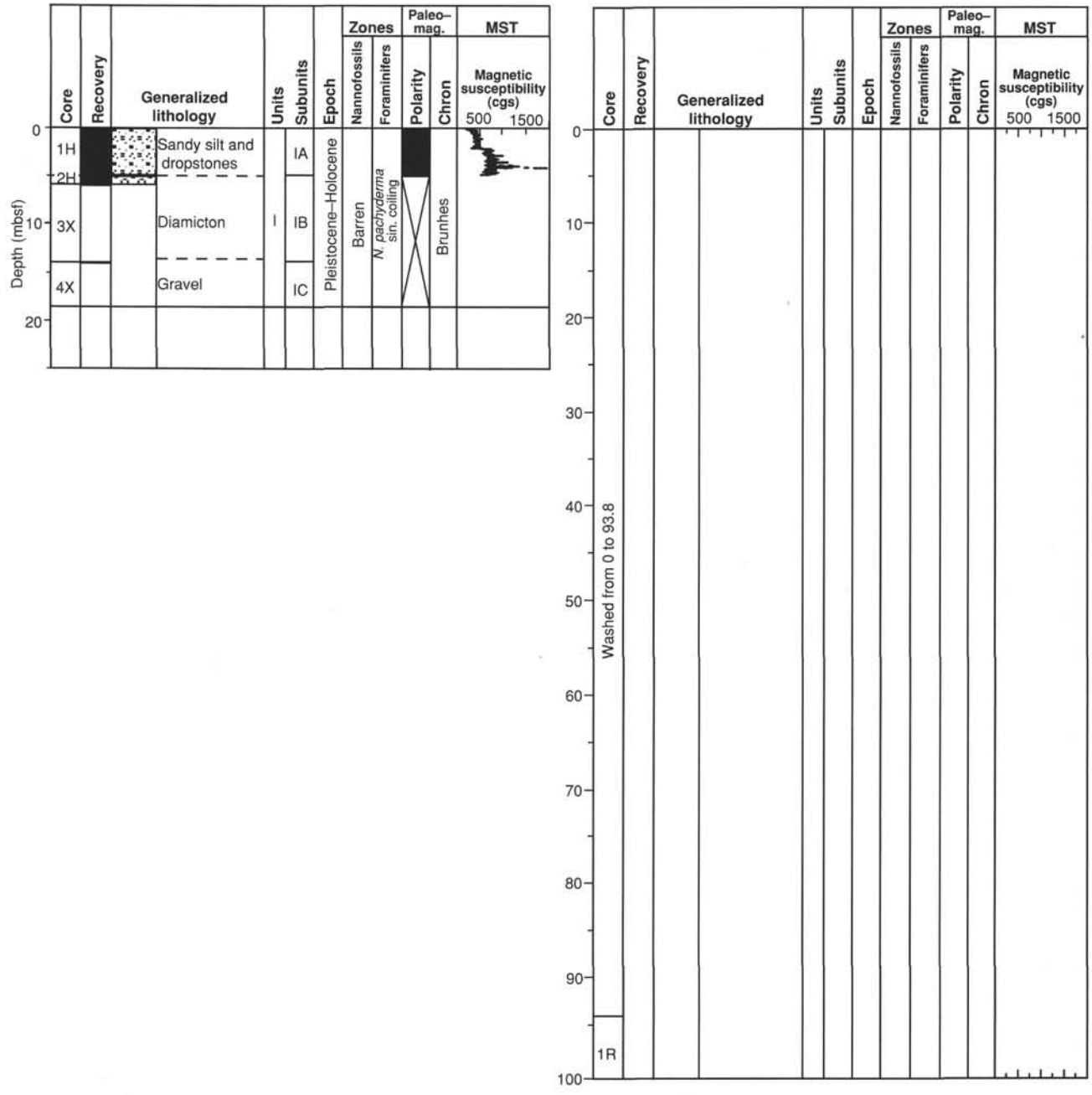

Figure 1. Site summary for Site 914.

A detailed study of benthic and planktonic foraminifers in Core 152-914A-1H was undertaken to provide a biostratigraphic framework for environmental evaluation of physical properties measurements. Fluctuations in sediment physical properties may be related to climatically induced changes in depositional environment. The benthic foraminifer assemblage indicates a transition from a glacial to interglacial environment in the upper 30 cm of the recovered sediments. Multisensor track (MST) data from the uppermost part of Unit I revealed marked changes in all physical properties. These pronounced changes within the Quaternary sediments include rapid downcore increases in wet bulk density, magnetic susceptibility, and natural gamma. Diamictons recovered in Core 152-914A-2H exhibit high shear strengths, which is consistent with subglacial compaction.

Core 152-914A-1H was analyzed for paleomagnetic properties in Hole 914A; below this core, recovery was minimal and most intervals showed excessive drilling disturbance. The core is of normal polarity. Correlation with the Brunhes Chron is proposed. Paleomagnetic data were obtained from four cores in Hole 914B (Cores 152-914B-13R and -15R to -17R). Core 152-914B-15R carries a reverse polarity magnetization. Core 152-914B-16R and the upper part of Core 152-914B-17R (down to Section 152-914B-17R-3, 75 cm) also are reversely magnetized. The lower part of Core 152-914-17R carries a normal polarity remanence. Biostratigraphic data suggest that the reverse polarity remanence of Cores 152-914B-15R and -16R probably represents a partial record of Chron C12r. Nannoplankton data from Core 152-914B-17R indicate an age range of 32 to 35 Ma. Thus, the downhole transition from reverse to normal polarity in Core 152-914B-17R may represent either the reversal between Chrons C12r and C13n or that between Chrons C13r and C15n.

Principal findings at Site 914 were as follows:

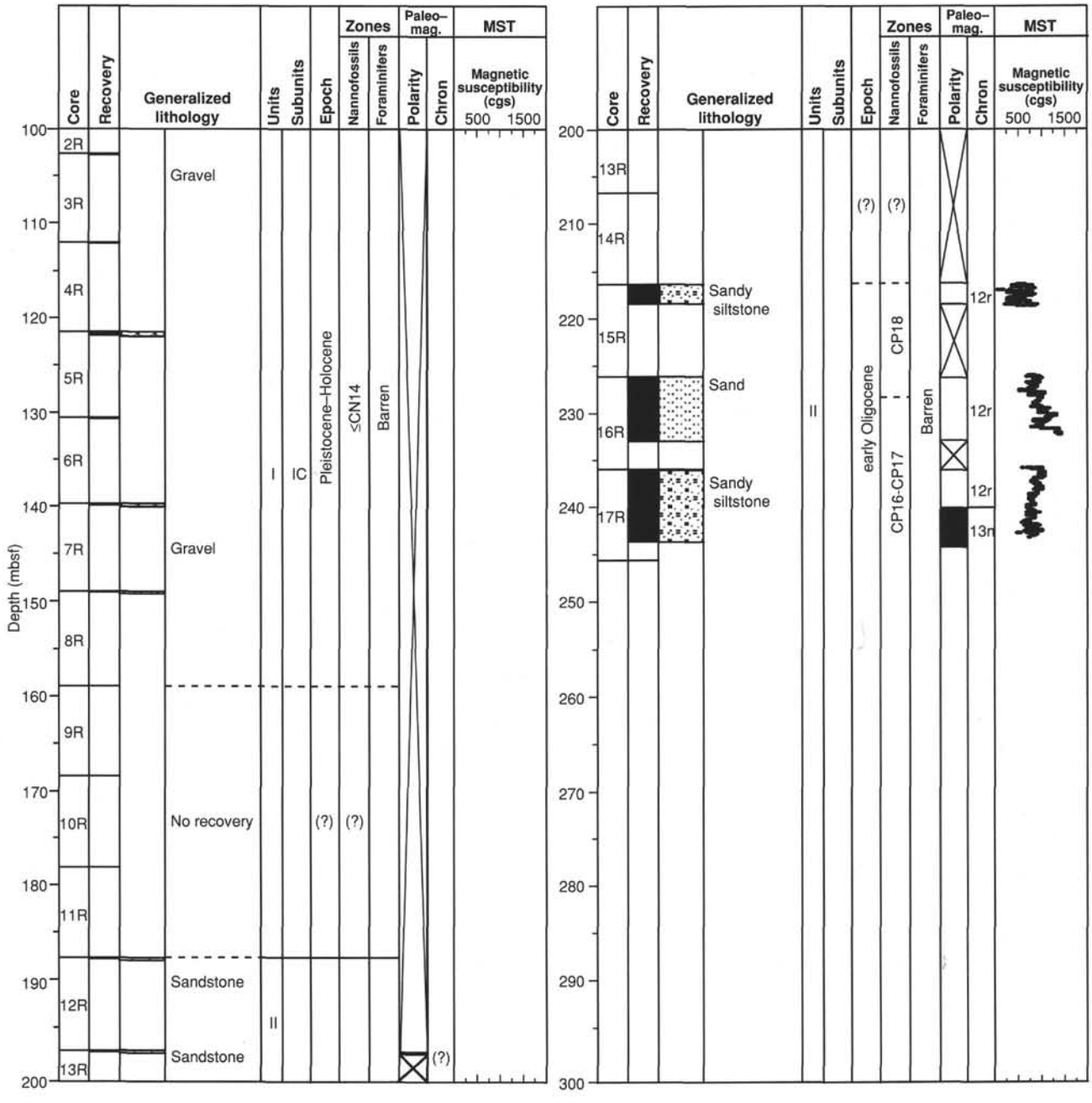

Figure 1 (continued).

1. The presence of diamicton confirms that wet-based glaciers advanced to at least this point on the shelf, about 60 km east of the present ice sheet. The tephra found in the uppermost part of the core will enable us to determine whether this advance pre-dates the latest (Weichselian) glaciation.

2. The benthic and planktonic foraminifers in the Quaternary and Holocene sediment illustrate changes in climatic conditions during glacial and interglacial periods.

3. The oldest sediment recovered at this site is latest Eocene-early Oligocene age, and it confirms that marine shelf conditions existed at that time. Benthic foraminifers indicate water depths of between 100 and 250 m at that time, thus providing a datum point for the subsidence study of the margin.

4. A marked hiatus exists between the early Oligocene strata and the Quaternary glaciomarine deposits.

OPERATIONS

Reykjavik Port Call

Leg 152 began when *JOIDES Resolution* arrived at Sundahofn Pier 411, Reykjavik, at 0700 hr (all times are in Universal Time Coordinated or UTC) on 24 September 1993. The port call was relatively light in terms of logistical and repair activities. In addition to the routine air and ocean freight, technical support personnel were available to service the Kappabridge and XRF equipment. Incoming Operations shipments of note included 10 RBI (5-C4 and 5-C7) rotary core barrel (RCB) bits and the Dril Quip 20/16 in. running tool.

The vessel took on 1519.8 MT of fuel, 860 gal of turbine-grade oil, and 953 MT of potable/drilling water. The time-determining item

for this port call was the replacement of the Nos. 2 and 3 crown sheave bearings, a job that lasted until the evening of 29 September. The auxiliary seawater cooling lines also were cleaned out during this port call.

The port shaft seal, which was found to be leaking during Leg 151, was inspected by divers in the port. No visible reason could be found for the leaking seal. It was decided to load up with additional turbine grade oil (860 gal) and continue the cruise as scheduled. The last line was away at 1230 hr on 28 September, and the vessel sailed for the first site.

Transit to Site 914

When the *JOIDES Resolution* had cleared Reykjavik harbor, a course was set nearly due west for the operating area. Initially, the weather was clear and cold, with occasional showers, but toward the evening hours, this turned to snow flurries. Gentle 8-ft swells from the south-southwest caused a gradual 3° to 4° roll. By the next day, swells had abated and the remaining transit was accomplished in calm seas and overcast skies.

At 0500 hr on 30 September, the ship slowed to 5 kt to deploy seismic gear and to conduct a short site survey. At 0726 hr, a Datasonics beacon (Model 354B, 16 kHz, serial number 758), modified to operate at a reduced source level (199 dB), was deployed. After the seismic gear was retrieved, the ship returned to location and was positioned on Site 914 by 0900 hr.

Site 914

The initial site of Leg 152 was on the continental margin of Southeast Greenland, approximately 23 nmi offshore and in approximately 530 m of water. The plans called for an advanced piston corer/extended core barrel (APC/XCB) hole to be drilled to refusal, followed by a rotary core barrel (RCB) hole, which was to be extended 50 m into basement. Sediments were estimated to be 420 m thick, and our ambitious basement objective called for coring 400 m into basalt. The third (RCB) hole of this site called for emplacement of a cased reentry cone. Logging was to be in two stages. The first logging run would be deployed in the pilot hole in sediment, with the second run planned solely for basement.

Upon coming on location, the crew was greeted with a spectacular view of the southeast coast of Greenland, illuminated by the rising sun. Large icebergs were observed heading south at various speeds, ranging from 1 to 3 kt. These icebergs appeared to be following a north-south channel, which was about 12 nmi west of our location. In addition, several large icebergs seemed to be grounded, with one large iceberg stuck on the seabed in 215 m of water about 10 nmi from the ship.

Hole 914A

The precision depth recorder (PDR) indicated that the corrected water depth, adjusted to sea level, was 533.4 m. A used RBI 11-7/16-in. bit was fitted to the bottom-hole assembly (BHA). The C-3 bit was lowered to 529.8 m, and the first APC core was "shot" at 1430 hr on 30 September. The depth of the seafloor was established at 533.8 m by direct pipe measurement (DPM), based upon the recovery of 5.01 m of clay-laden sediments. APC coring was abruptly halted when the second core did not produce a full stroke. When the core barrel was retrieved, we found that the liner was shattered, indicating a high-impact landing on firm sediment. After the core was dug out of the core barrel, we found that it measured about 6.6 m.

Instead of employing the advance-by-recovery method to record our progress, we recorded the amount of penetration at 1 m because washing down the interval represented by Core 152-914A-2H indicated a very hard zone after penetrating only 1 m. Apparently, when the core barrel was retracted, it sucked in clay from the surrounding sediments.

XCB-coring was initiated, but was terminated after two cores that succeeded in recovering only 0.3 m of glacial till, while penetrating 12.6 m in a lethargic 4 hr. The BHA was retrieved, and the hole terminated when the bit cleared the rig floor at 2200 hr on 30 September. The coring sequence at Hole 914A, as well as at other holes at Site 914, is shown in Table 1.

Hole 914B

After a call to TAMU/ODP management, who approved our drilling to 100 m to be followed by continuous RCB coring, an RCB BHA was made up with a bit release. The pipe was run in the hole, and Hole 914B was spudded with a center bit in place at 0130 hr on 1 October. After drilling ahead for 14.5 hr at an average rate of penetration (ROP) of 8.6 m/hr, the core barrel was dropped and coring initiated at 93.8 mbsf at 1500 hr on 1 October. During drilling, a 10-bbl high-viscosity mud sweep was done after every connection. No problems were encountered in the hole when drilling through the glacial till.

RCB-coring advanced to 139.5 mbsf through glacial material having low recovery, with a 10-bbl high-viscosity slug pumped after every connection. At 116 mbsf, an extra 20-bbl high-viscosity pill was circulated when a probable plugged bit caused the pressure to rise temporarily to 1000 psi. The drilling crew felt that the bit would clear itself, and after the next core, the pressure did return to 400 to 800 psi. The ROP for this interval ranged from 18 to 37 m/hr.

A problem arose with the drill string when the bit was at 187.2 mbsf, immediately after making a connection. After lifting the pipe off the slips, we found that the drill string could not be lowered down the hole. With both knobbies and a newly added joint of pipe in the derrick, working the pipe upward was not possible because the compensator was locked. In addition, no movement down the hole was possible because the drill string was stuck by the formation. Rotation was possible with erratic high torque (300–400 A). During this operation, circulation was maintained.

The ship was offset 165 ft forward, forcing the pipe connection to lower to the slip level. The connection then was broken, a joint of pipe removed, and the pipe pulled up approximately 10 m. After an additional 20-bbl high-viscosity pill was circulated, the pipe was successfully worked free. The joint of pipe that had been laid down was added once more to the drill string and coring proceeded.

By 0500 hr on 2 October, a storm from the north, which had started the previous evening, had built to sustained winds of 38 to 40 kt, with gusts to 60 kt. Although the sea's swells were 10 to 14 ft, operations continued. As coring advanced down the hole, the weather deteriorated. By the time coring reached a depth of 245.0 mbsf, the storm had begun to push the vessel to her operational limits. Winds now had reached a sustained 50 kt, with frequent gusts that exceeded 70 kt. The sea's swells reached 25 ft, causing the ship to roll 3° to 5°, with pitch between 2° and 5°. Eight engines were online, producing an average of 8 MW, with peak loads exceeding 10.8 MW. The dynamic positioning system (DPS) was commanding 80% of available power merely to hold the ship on station. Large waves impacting the vessel caused an immediate horizontal offset of 100 ft (18% of water depth), which required that the overloaded power plants increase output to the thrusters to move the vessel back over the location. In addition, the heave compensator was frequently fully stroked out and at the limit of its capability. We decided to terminate operations and to pull out of the hole to wait for the storm to abate. The storm lasted through the evening, with no loss of wind strength. At the height of the storm, the seas were 40 to 60 ft with green water breaking over the ship's bow.

At 1030 hr on 3 October, the storm had lessened to allow the drilling crew to pull the BHA to the surface. Although the original bit still looked like new (with only 16 hr rotation time), another new C-4 bit was made up, the MBR was replaced, and three more drill collars were added to the BHA to anticipate the additional weight on bit required when coring basalt. By 1445 hr the same day, the BHA was

Table 1. Coring summary, Site 914.

Core	Date (1993)	Time (UTC)	Depth (mbsf)	Length cored (m)	Length recovered (m)	Recovery (%)
152-914A-						
1H	Sept. 30	1535	0.0–5.0	5.0	5.01	100.0
2H	Sept. 30	1615	5.0–6.0	1.0	6.57	657.0
3X	Sept. 30	1750	6.0–14.0	8.0	0.20	2.5
4X	Sept. 30	1900	14.0–18.6	4.6	0.10	2.2
Coring totals:				18.6	11.88	63.9
152-914B-			*** Drilled 0– 93.8 mbsf ***			
1R	Oct. 1	1600	93.8–99.0	5.2	0.00	0.0
2R	Oct. 1	1740	99.0–103.0	4.0	0.00	0.0
3R	Oct. 1	1930	103.0–112.1	9.1	0.12	1.3
4R	Oct. 1	2130	112.1–121.3	9.2	0.13	1.4
5R	Oct. 1	2300	121.3–130.4	9.1	0.54	5.9
6R	Oct. 2	0015	130.4–139.5	9.1	0.15	1.7
7R	Oct. 2	0130	139.5–148.7	9.2	0.21	2.3
8R	Oct. 2	0230	148.7–158.5	9.8	0.18	1.8
9R	Oct. 2	0330	158.5–168.0	9.5	0.00	0.0
10R	Oct. 2	0430	168.0–177.6	9.6	0.00	0.0
11R	Oct. 2	0530	177.6–187.2	9.6	0.00	0.0
12R	Oct. 2	0755	187.2–196.8	9.6	0.14	1.5
13R	Oct. 2	0920	196.8–206.5	9.7	0.14	1.4
14R	Oct. 2	1030	206.5–216.1	9.6	0.00	0.0
15R	Oct. 2	1200	216.1–225.8	9.7	1.94	20.0
16R	Oct. 2	1310	225.8–235.5	9.7	6.64	68.4
17R	Oct. 2	1415	235.5–245.0	9.5	7.59	79.9
Coring totals:				151.2	17.78	11.8
Drilled:				93.8		
Total:				245.0		
152-914C			*** Drilled 0–224.0 mbsf ***			
No recovery						

run down to 339.8 m. Our original plan was to try to reenter Hole 914B, even though no free-falling funnel (FFF) had been deployed. When the surge though the moon pool proved too rough to launch a vibration-isolated television camera (VIT), we decided that it would be better to offset the vessel 5 m east, to spud a new hole, and to drill down to 225 mbsf to resume coring.

Hole 914C

After a total of 22 hr was spent waiting on the weather, operations again resumed at Site 914 at 1845 hr, when the pipe was lowered to 508.8 m. Hole 914C was spudded with the RCB and center bit at 2000 hr on 3 October. While drilling in Hole 914B had been relatively free of hole problems, Hole 914C required many short trips and extra mud flushes to keep the hole open. The hole was drilled to 224 mbsf, and the center bit retrieved. When dropping the first core barrel at 1915 hr on 5 October, circulation was immediately lost, and the drill string could not be rotated. The core barrel was brought up a few feet, which allowed for a limited amount of circulation (80 spm and 1000 psi). A 20-bbl high-viscosity pill was circulated without any effect. Frequent overpulls of 100,000 lb (100 kips) were not effective in freeing the drill string. During one of the overpulls, the ship heaved with the swell and added an additional overpull so that the string was subjected to a total of 260 kips over the 240 kips of string weight (500 kips total weight). The drill string immediately came free, and the pump pressure quickly dropped to 200 to 300 psi with 80 spm.

After pulling back to 204.0 mbsf, the pipe was lowered to 209.0 mbsf, where we found an apparent 15.0 m of fill. The core barrel was retrieved and the center bit dropped. No pressure change was observed, indicating a successful landing of the inner barrel. The drill string was picked up approximately 10 m, after the wireline had been run in and picked up the inner barrel. The center bit was again run, but did not land at bit level as expected. Instead, it landed at the bottom of the hole at 209 mbsf. This strongly suggested that the bit was no longer on the end of the drill sting. We had no choice but to pull out of the hole and inspect the damage. An FFF was not deployed because of the high probability that the bit was missing. This was confirmed when the BHA arrived on deck at 1200 hr on 3 October. The bit and mechanical bit release (MBR) were missing, and it appeared that the bit release had been forced apart from the dogs, which were still mounted in the top connector. The bit, bit seal, lower support bearing, float valve, and the bit disconnect were left in the hole.

The site was abandoned in favor of moving approximately 2 nmi west-northwest, where the glaciomarine sediments were thinner and the basement closer to the mud line. The beacon was turned off as the vessel moved off location in case a return to the site was necessary. We expected to make a quick stop here to pick up the beacon when concluding operations in the area.

LITHOSTRATIGRAPHY

Introduction

Site 914 is the most seaward of four sites (914, 915, 916, and 917) drilled along a 6-km-long transect at the outer, middle shelf of the East Greenland Margin. It is located in 533 m of water, approximately 25 km from the shelf edge. Three holes were drilled at this site, with recovery from the first two holes only. We divided the recovered section into two lithologic units (Table 2, Fig. 2): an upper, Quaternary age, glaciogenic deposit (lithologic Unit I) and an underlying, lower Oligocene–upper Eocene mixed volcaniclastic and siliciclastic shelf deposit comprising bioturbated, sandy silt and mud with interbeds of silty sand (lithologic Unit II).

Lithologic Unit I comprises three glaciogenic subunits. We differentiated these subunits mainly by degree of compaction and presence or absence of matrix. The sediments are not compacted in the upper Subunit IA, but are highly compacted in the medial Subunit IB. No matrix was recovered in the lower Subunit IC.

Lithologic Units

Lithologic Unit I: Glaciomarine mud with dropstones, diamicton (till), and gravel
Interval: Sections 152-914A-1H-1 to 152-914A-4X-CC, and 152-914B-3R-CC to 152-914B-8R-CC
Depth: 0–158.5 mbsf
Thickness: 158.5 m
Age: Quaternary

Table 2. Summary of lithologic units, Site 914, East Greenland Margin.

Lithologic unit	Lithology	Depth (mbsf)	Core intervals	Thickness (m)	Age
I	Glaciomarine mud with dropstones and diamicton (till)	0–158.5	152-914A-1H-1, 0 cm, to 152-914A-4X-CC, and 152-914B-3R-CC to 152-914B-8R-CC	158.5	Quaternary
IA	Glaciomarine mud with dropstones	0–5	152-914A-1H-1, 0 cm, to 152-914A-1H-CC	5	Quaternary
IB	Compacted diamicton (till)	5–14.0	152-914A-2H-1, 0 cm, to 152-914A-3X-CC	9	Quaternary
IC	Gravel	14.0–158.5	152-914A-4X and 152-914B-3R to -8R-CC	144.5	??
Gap	No recovery	158.5–187.2	152-914B-9R-CC to 152-914B-11R-CC	28.7	??
II	Sandy silt with silty sand interbeds	187.2–245.0	152-914B-12R-CC, 0 cm, to 152-914B-17R-CC	57.8	Oligocene to late Eocene

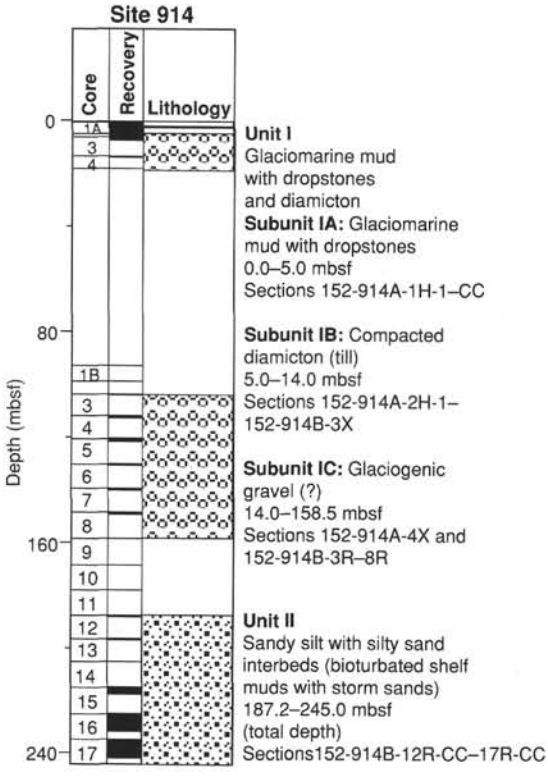

Figure 2. Lithostratigraphic summary of Site 914, East Greenland Margin.

This lithologic unit comprises three subunits. The upper Subunit IA comprises 5 m of Holocene glaciomarine sandy silt with dropstones, underlain by Subunit IB, with 9.0 m of Quaternary compacted diamicton. The lower Subunit IC was recovered as isolated cobbles of igneous, metamorphic, or sedimentary rocks, with no matrix over a 144.4-m-thick interval. These lower gravels were probably recovered from older glaciomarine deposits or, in part, from subglacial channel deposits associated with the glaciation recorded by Subunit IB. Downhole contamination by dropstones from Subunits 1A and 1B may also contribute to the cobbles recovered in Subunit 1C.

Lithologic Subunit IA: Glaciomarine mud with dropstones
Interval: Sections 152-914A-1H-1 to 152-914A-1H-CC
Depth: 0–5.0 mbsf
Thickness: 5.0 m
Age: Quaternary

This lithologic subunit comprises sandy silt, silty sand, sandy silt with dropstones, and sandy mud with dropstones. The top 5 cm is a sandy nannofossil mixed sediment, with 40% calcareous nannofossils, many preserved as whole coccolithophorids. Biogenic detritus reaches a maximum of 50% of the sediment in the upper 5 cm of the core, but decreases dramatically downcore, totaling only 15% in the sediment over the next 20 cm, and less than 10% thereafter. Siliceous microfossils are dominated by sponge spicules. Diatoms and radiolarians comprise a maximum of 1% of the sediment in this interval. Below the top 5 cm, foraminifers occur as fragments only, making up no more than 1% of the sediment.

An ash-rich zone occurs in Section 152-914A-1H-1 at a depth of 30 to 35 cm. The ash is not visible on the surface of the sectioned core, but was recognized during sampling for foraminifers and in a smear slide. The ash makes up about 5% of the sediment and consists primarily of vesicular basaltic micropumice and bubble wall fragments. Most shards are from 30 to 60 µm in diameter. The shard edges appear angular and fresh. No evidence of superhydration was observed in the smear slide. A few platy bubble wall shards of colorless tephra of similar size are also present in the sediment. Given the bimodal character of the tephra zone and its occurrence near the top of the first core, it is possible that this unit is "ash zone I" (Ruddiman and Glover, 1972), found widely in the North Atlantic region. This marine tephra deposit might correlate with similar land-based deposits in Norway (the Vedde ash) and in Iceland (the Skóga tephra) (Mangerud et al., 1984; Norddahl and Haflidason, 1992). The Vedde ash and Skóga tephra are about 10,600 yr old. This initial interpretation will be confirmed or modified on the basis of shore-based chemical analyses.

The sand fraction of lithologic Subunit IA is dominated by quartz, but has significant contributions of green and blue-green amphibole, feldspar, pyroxene, and lithic fragments. Blue-green amphibole in the sand fraction indicates a metamorphic provenance as one contributor to this sediment. The lithic fragments are similar to the larger gravel clasts recovered in lithologic Subunit IC (Table 3). Volcanic glass and dolomite each make up about 1% of the sediment. The zeolite phillipsite is present in trace amounts. As the volcanic glass here is very fresh and because it probably took phillipsite more time to form than the few thousand years that it took this sediment to accumulate, phillipsite may have been derived from an updip exposure of the underlying lithologic Unit II, which is rich in phillipsite. X-ray diffraction (XRD)

Table 3. Summary of hand-specimen descriptions of gravel recovered in lithologic Subunit IC, Site 914, East Greenland Margin.

Rock type	Number	Comments
Basalt	10	Both altered and relatively fresh.
Metabasalt	1	Blackish-green in color.
Diabase (dolerite)	1	
Gabbro	2	
Andesite	1	
Felsic gneiss	5	Predominantly quartz and feldspar.
Garnet amphibolite	1	
Serpentinite	1	
Quartz diorite	1	Metamorphosed.
Granite	1	Metamorphosed.
Quartzite	1	
Metaconglomerate	1	Relict large clasts remain.
Metapelite	1	Light gray and nonbedded.
Siliceous metasediment	1	Some recrystallized small clasts.

results of the silt + clay fraction reveal a rock flour of amphibole, mica, quartz, plagioclase, phillipsite, and dolomite. No clay minerals are present because chemical weathering was minimal on Greenland throughout the Quaternary, and shales, which could provide detrital clay, were not a significant source for this unit.

The sediment is very soft and shows no bedding. Dropstones occur more or less randomly, in no preferred orientation, in the soft sediment (Fig. 3). They are principally angular and range from sand size to at least the width of the core (6 cm) and make up a variety of mainly metamorphic and igneous rocks. Basalt, dolerite, granitic gneiss, gabbro, quartz diorite, and quartzite clasts were identified.

Lithologic Subunit IB: Compacted diamicton (till)
Interval: Sections 152-914A-2H-1 to -3X-CC
Depth: 5.0–14.0 mbsf
Thickness: 9.0 m
Age: Quaternary

Diamicton was recovered in Cores 152-914A-2H and -3X, and some fragments were recovered in Cores 152-914B-7R and -8R. This sediment exhibits a preferred fabric (Fig. 4) and is very compact compared to the sediment just above it (see "Physical Properties" section, this chapter). Gravel-size clasts are scattered randomly through the sediment. Most are angular, but a few are rounded. We interpret the preferred fabric and the density of the sediment as being the result of the compressive effects of an overriding glacier (see more detailed discussion in "Lithostratigraphy" section, "Site 916" chapter, this volume). Some red sandstone clasts in this sediment were not present in the overlying subunit and may have been derived from deeper within the interior of Greenland or from the sedimentary basins in Northeast Greenland.

The sand fraction is dominated by quartz and contains abundant feldspar, lithic fragments, and accessory minerals, such as amphibole and pyroxene. XRD results from the silt + clay fraction are similar to those of Subunit IA, except for the absence of mica in this subunit. The fines of this sediment make up a rock flour composed of quartz, plagioclase, and amphibole. As for Subunit IA, no clay minerals are present. More till was recovered at Site 916, and a more detailed description of it can be found in that site chapter.

Lithologic Subunit IC: Glaciogenic gravel
Intervals: 152-914A-4X and 152-914B-3R-CC, to 152-914B-8R-CC
Depth: 14.0–158.5 mbsf
Thickness: 144.5 m
Age: unknown, presumed Quaternary

This interval is identified by large drilling fragments of igneous and metamorphic rocks with no matrix material recovered. We think that these fragments are derived from either the diamicton, from older glaciomarine deposits, or, in part, from subglacial channel deposits associated with the glaciation recorded by Subunit IB. Contamination from sediments higher in the borehole cannot be excluded.

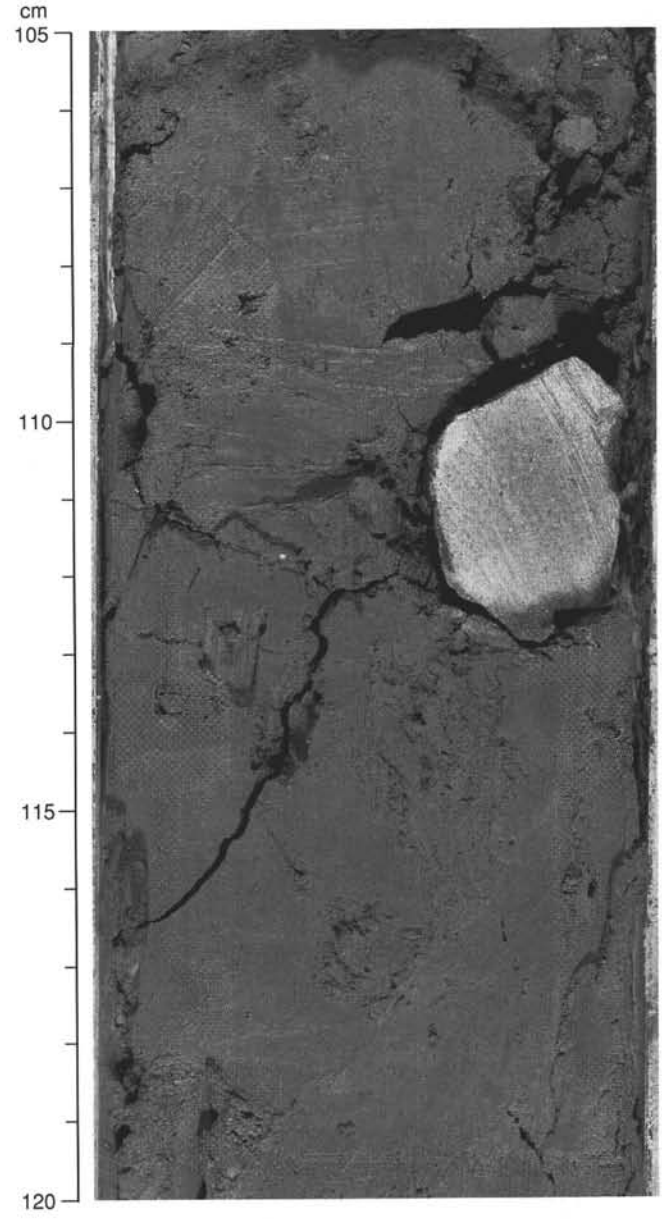

Figure 3. Photograph of lithologic Subunit IA, glaciomarine mud with dropstones, interval 152-914A-1H-3, 105–120 cm. Matrix of silt has sand- to gravel-sized fragments floating throughout. Calcareous nannofossils, planktonic and benthic foraminifers, and sponge spicules are common components, but other siliceous microfossils occur only as rare fragments.

Twenty-eight clasts were described by use of hand lens (Table 3). Thin sections of five clasts also were examined with a petrographic microscope (Table 4). We compared the lithologies of the clasts with rocks present on the East Greenland Margin to identify possible source areas. Clast compositions indicate that glaciers eroded source terranes from several regions of eastern Greenland. The source areas include regions composed of Precambrian(?) gneiss, amphibolite, and metasedimentary rocks, and regions of Tertiary volcanic and plutonic rocks. Precambrian rocks occur along the coastline of East Greenland just west of the drill site. However, at the present time, the nearest extensive outcrops of Tertiary volcanic rocks are in the Kangerdlugssuaq region (68°N) more than 500 km north of the drill site. However, small

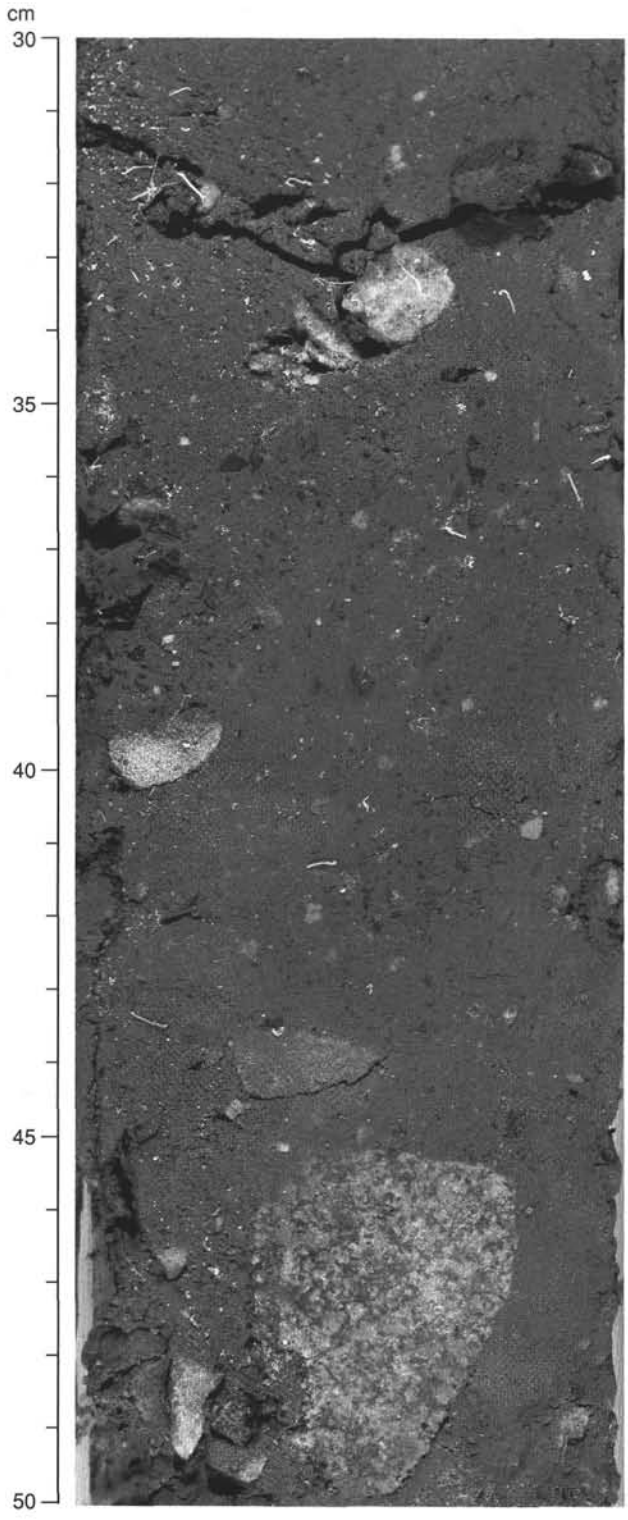

Figure 4. Photograph of lithologic Subunit IB, compacted diamicton (till), interval 152-914A-2H-2, 30–50 cm. Note poor sorting, polymict aspect of sediment and angular granitic fragment, 45 to 50 cm. Some oriented fabric is visible on the left side of the core, 31 to 39 cm, suggestive of the plowing effect of a grounded glacier depositing this sediment.

Table 4. Composition of five rocks (estimated percentage for igneous rocks) from Hole 914B, determined by petrographic microscope from thin sections.

Core interval (cm)	Rock type	Minerals	Percentage (%)
152-914B-5R-1, 20–25 (Piece 4)	Quartz diorite	Plagioclase	40
		Quartz	30
		Hornblende	20
		Orthoclase	5
		Iron oxides	1
		Epidote	4
		Garnet	tr
		Sphene	tr
		Calcite	tr
		Apatite	tr
152-914B-5R-1, 40–45 (Piece 7)	Olivine gabbro	Plagioclase	45
		Clinopyroxene	35
		Olivine	12
		Iron oxides	8
152-914B-5R-1, 65–69 (Piece 11)	Metapelite	Quartz	
		Feldspar	
		Hornblende	
		Opaque minerals	
		White mica	
152-914B-6R-1, 8–13 (Piece 2)	Ferrobasalt	Plagioclase	45
		Clinopyroxene	30
		Iron oxides	25
		Epidote	tr
152-914B-7R-CC, 13–17 (Piece 3)	Granite	Plagioclase	40
		Quartz	35
		Biotite	10
		Hornblende	5
		Orthoclase	5
		Epidote	tr
		Calcite	tr
		White mica	tr
		Sphene	tr

Note: tr = trace amounts.

patches of Tertiary volcanic and plutonic rocks are present along the coast farther south (66°N) and subcrop at the seafloor west of the drill site. These could be the remnants of much larger areas of outcrops that have been subsequently removed by erosion. Clearly, both Tertiary basalts and Precambrian continental basement were being eroded to form this sediment.

Lithologic Unit II: Sandy silt with silty sand and sandstone interbeds
Interval: 152-914B-12R-CC, 0 cm, to 152-914B-17R-CC
Depth: 187.2–245.0 mbsf (t.d.)
Thickness: 57.8 m (base not recovered)
Age: early Oligocene and late Eocene

The dominant lithology in this unit is a greenish-black, massive, homogeneous sandy silt that has been extensively bioturbated (Fig. 5). Sand-filled burrows are evident intermittently. This unit contains quartz, plagioclase, amphiboles (some blue-green), pyroxene, garnet, mica, and lithic fragments of basalt. Pyrite, basalt fragments, amphibole, pyroxene, wood fragments, and glauconite all contribute to the dark green color of the sediment. Phillipsite is abundant in the lower part of the unit, where it constitutes up to 20% of the sediment. This zeolite is usually produced by the alteration of volcanic glass in seawater (e.g., Biscaye, 1965). The presence of blue-green amphibole, garnet, and muscovite indicates erosion of a metamorphic source terrane, as is the case with lithologic Subunit IIA at Site 915 (see "Lithostratigraphy" section, "Site 915" chapter, this volume). XRD analysis of the bulk sediment reveals phillipsite, quartz, calcite, and feldspar. The only clay mineral present is smectite.

Calcareous sandstones (Fig. 6) in four cores from Hole 914B occur in Sections 152-914B-12R-CC and -13R-CC and within the lower Oligocene black sandy silt (intervals 152-914B-15R-1, 0–19 cm, and 152-914B-16R-3, 86–99 cm). These sandstones are dark gray to olive gray and consist predominantly of sand-sized grains in

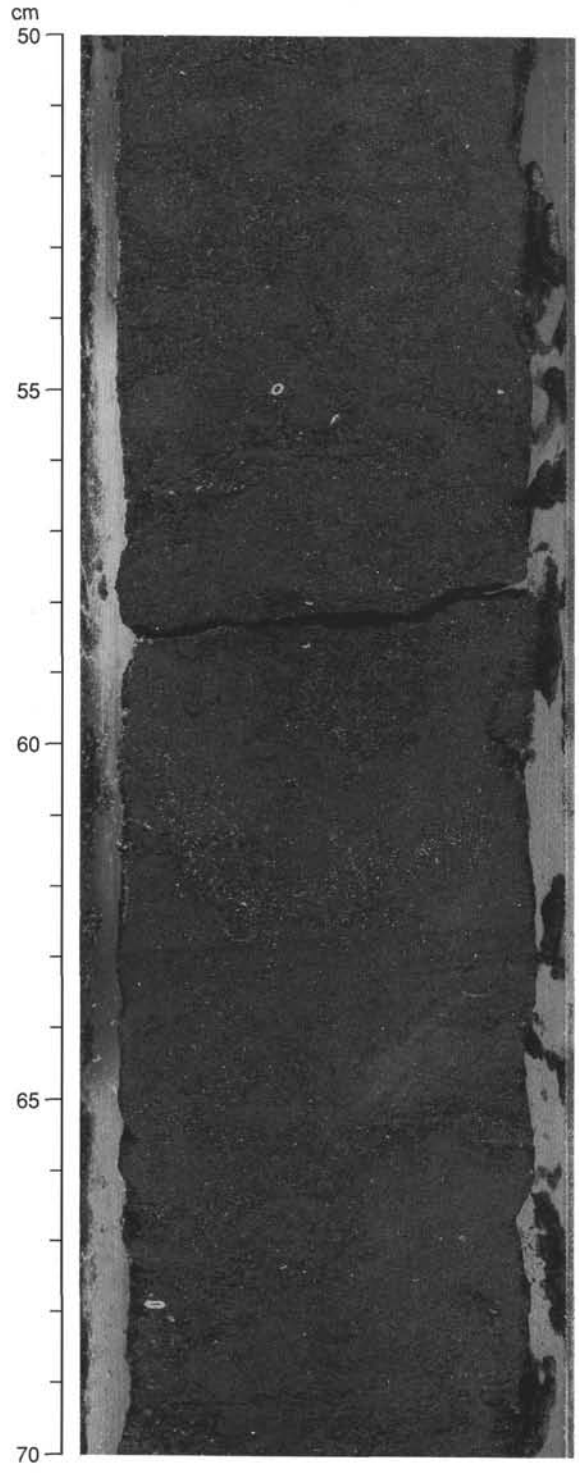

Figure 5. Photograph of black silty sand and sand from lithologic Unit II, interval 152-914B-16R-1, 50–70 cm. Close inspection of this photograph reveals sandy burrows worked into the silty matrix (60–62 cm) and silt worked into a sandier matrix (52–56 cm). White spots and circles are scattered molluscan fragments. A few laminae and cross laminae are faintly visible between 62 and 65 cm, but most bedding and lamination have been destroyed by bioturbation.

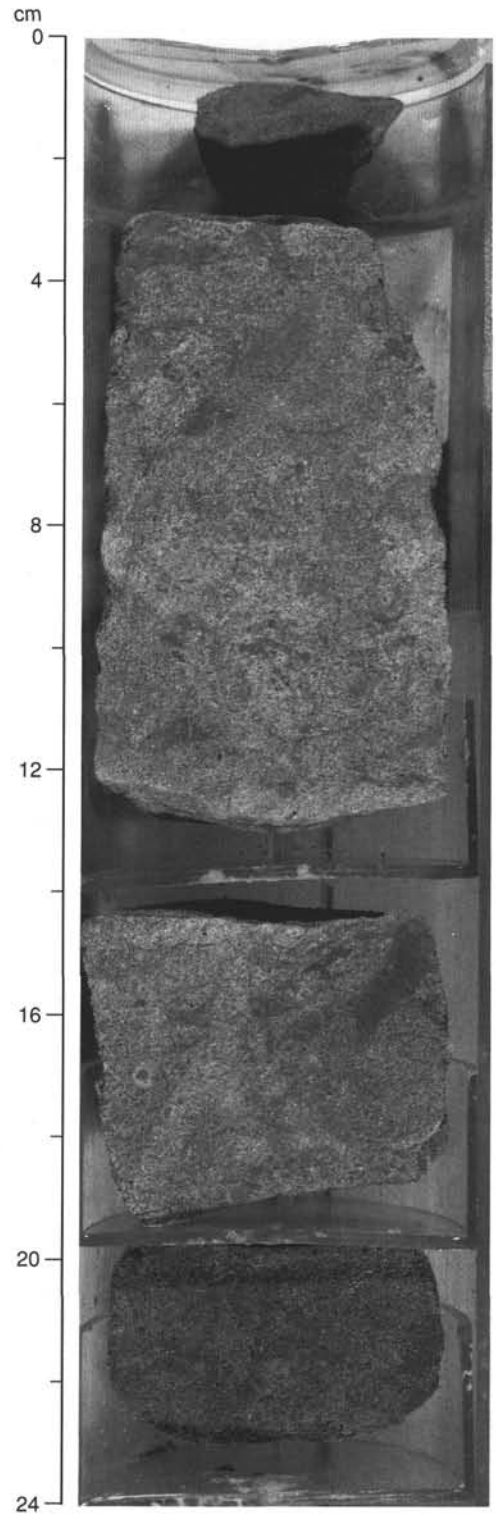

Figure 6. Photograph of a sandy interbed of lithologic Unit II, within black silty sand, interval 152-914B-15R-1, 0–24 cm. Most, but not all, of the sand interbeds are calcite-cemented, as shown here. All sandy intervals are highly anisotropic, intensely bioturbated, and show elevated levels of glauconite pellets over the intervening silty sediment, indicating deposition by high energy events, such as storms, followed by a hiatus during which the rapidly deposited sediment was intensively bioturbated.

a calcite cement. The top of the bed in interval 152-914B-16R-3, 86–99 cm, is heavily burrowed, while the bottom part is not burrowed, suggesting that the bed was deposited during one event. Based on the occurrence of similar sandstone in Cores 152-914B-15R and -16R, we surmise that the sandstone fragments recovered in the core-catcher samples of Cores 152-914B-12R and -13R are probably individual beds within an unrecovered softer and less lithified sequence.

We described and point-counted (Table 5) one thin section of the calcareous sandstone (interval 152-914B-13R-CC, 10–14 cm). It consists of moderately well-sorted grains enclosed within a calcite cement. The grain shapes are subangular to well-rounded, with quartz and quartzite composing about 70% of the sand-sized grains. One complete, but partly recrystallized, foraminifer was identified in the thin section.

In smear slides, the cement appears to have been derived in part from the dissolution of calcareous nannofossils as well as foraminifers, as only a few robust forms are present. Molluscan fragments, echinoid spines, benthic foraminifers, and wood fragments are scattered throughout the sediment. Glauconite pellets appear as foraminifer molds and fecal pellet replacement and are enriched in the sand beds relative to the enclosing site. No sedimentary structures are evident in the sand beds aside from the intense bioturbation. Enrichment of the calcareous sandstone in quartz relative to the enclosing black silt suggests a more mature source for these sandbeds and/or different depositional regimes. The anisotropy of these intervals is high, which indicates rapid deposition from very strong currents, such as might be encountered in strong storms (see "Physical Properties" section, this chapter). This period of rapid deposition was followed by a hiatus during which the sandy floor was intensely bioturbated and later cemented.

The presence of marine fossils and glauconite pellets indicates a marine origin for lithologic Unit II. The fine grain size and extensive bioturbation suggest a mid- to outer-shelf environment of deposition, where mud that eroded from the continent accumulated at a rate slow enough to encourage benthic organisms to thoroughly bioturbate the sediment and for glauconite pellets to form. Sandy interbeds suggest periodic episodes of increased current activity, probably related to large storms. These punctuated an otherwise low-energy regime, with most of the sediment accumulating below wave base.

Summary

Unit I is a thick, Quaternary age, glaciogenic deposit comprising an upper 5 m of glaciomarine sandy silt with dropstones (Subunit IA), a middle 9.0 m of subglacially derived till (Subunit IB), and a lower 144.5 m of probable glaciogenic moraine or outwash plain gravel (Subunit IC). These sediments overlie a lower Oligocene–upper Eocene mid- to outer-siliciclastic shelf deposit at Site 914. The objective of describing the Greenland glaciation history, was advanced at this site by the recovery of the Quaternary lithologic Unit I, as we now have direct evidence that wet-based glaciers advanced to at least this point on the shelf, about 60 km from the edge of the present ice sheet.

Another objective for this site was to determine the age of the regional unconformity. The entire Pliocene-upper Oligocene section is missing at this site.

The lower Oligocene-Eocene sediment (lithologic Unit II) is bioturbated, glauconitic, mixed volcaniclastic and siliciclastic shelf mud with sandy interbeds. The sands are acoustically highly anisotropic, indicating rapid deposition from very strong, probably storm-induced currents.

BIOSTRATIGRAPHY

Calcareous Nannofossils

Sample 152-914A-1H-1, 20 cm, contains abundant nannofossils that have been moderately preserved. The species present include *Coccolithus pelagicus, Calcidiscus leptoporus, Emiliania huxleyi,* and *Gephyrocapsa* spp. On the basis of the common occurrence of *E. huxleyi*, this sample can be correlated with oxygen isotope stages younger than stage 4 (80 ka). Samples 152-914A-1H-CC through -3H-CC are barren of calcareous nannofossils. Sample 152-914B-8R-CC contains a mixture of nannofossils of different ages, including Cretaceous, Paleogene, and Pleistocene species. Apparently, these have been reworked in this glaciomarine sediment. The youngest species identified is *Gephyrocapsa* sp. (>4.5 µm), which indicates that the sediment is younger than 1.7 Ma.

Sample 152-914B-15R-CC contains a lower Oligocene assemblage (Fig. 7). The presence of *Reticulofenestra daviesii, R. umbilicus,* and *Chiasmolithus altus* in the absence of *Isthmolithus recurvus* indicates an age of about 31 to 32 Ma. Sample 152-914B-16R-2, 31 cm, also contains these age-diagnostic species. Samples 152-914B-16R-CC and -17R-CC contain all the above species in addition to *Isthmolithus recurvus*, while *Reticulofenestra reticulata* is absent. These assemblages indicate a latest Eocene–early Oligocene age (Fig. 7).

Planktonic Foraminifers

Planktonic foraminifers generally are absent from sediments at Site 914, except in the uppermost part of the sequence (Cores 152-914A-1H, -2H, -3X), where they are rare and moderately preserved. Samples 152-914A-1H-CC, -2H-CC and -3X-CC contain a few sinistrally coiled specimens of *Neogloboquadrina pachyderma*, which range from the lower Pleistocene to Holocene (Fig. 8). One specimen of *Globigerina bulloides* is recorded in Sample 152-914A-2H-CC.

The zonation of Spiegler and Jansen (1989), based on neogloboquadrinids, can be applied to sediments from Site 914. These assemblages thus may be attributed to the *Neogloboquadrina pachyderma* sinistral coiling Zone, which has an age range of Pleistocene to Holocene.

Benthic Foraminifers

Benthic foraminifers were recorded in Samples 152-914A-1H-CC, -2H-CC, and -3X-CC, and in 152-914B-15R-CC, -16R-CC, and -17R-CC. Benthic foraminifers constitute about half of the total foraminiferal assemblage within the Quaternary succession (Samples 152-914A-1H-CC, -2H-CC, and -3X-CC). Their preservation over this range is moderate. The foraminiferal assemblages are characterized by the occurrence of *Cassidulina teretis* and *Elphidium excavatum. Cassidulina teretis* was a dominant species during Pliocene to Pleistocene glacial intervals of the North Atlantic region (Murray, 1984).

Benthic foraminifers contribute 85% of the total foraminiferal assemblage within the recovered Paleogene sediments (Samples 152-914B-15R-CC and -16R-CC). Their preservation is poor over this interval. Samples 152-914B-15R-CC and -16R-CC contain rare benthic foraminifers. *Alabamina wilcoxensis, Cibicidoides alleni, Gyroidina* sp., and *Lenticulina* sp. were identified in Sample 152-914B-15R-CC. This fauna resembles that reported in DSDP Cores 48-403-27R and -28R by Murray (1979), who suggested a paleowater depth of 100 to 250 m. Sample 152-914B-16R-CC contains *Anomalinoides nobilis, Cibicidoides* sp., *Oridorsalis ecuadorensis*, and *Oridorsalis* sp. This assemblage was identified in DSDP Sample 81-553A-11-6, 52 cm, by Murray (1984), who suggested a paleowater depth of 75 to 200 m. Sample 152-914B-17R-CC is barren of benthic foraminifers.

A more detailed study was performed on benthic and planktonic foraminifers in six samples from Sections 152-914A-1H-1 and -1H-2 to provide a refined biostratigraphic framework for the glacial/interglacial fluctuations. Benthic foraminifer specimens also were counted to quantify the relative abundance of each species in the samples.

The following samples were analyzed for their faunal content: 152-914A-1H-1, 0–2 cm, 32–35 cm, 95–97 cm; -1H-2, 83–85 cm, 96–98 cm, and 135–137 cm. Sample 152-914A-1H-1, 32–35 cm, was taken within an interval where high abundances of basalt glass fragments had been found. Abundances of benthic fauna are shown in Table 6.

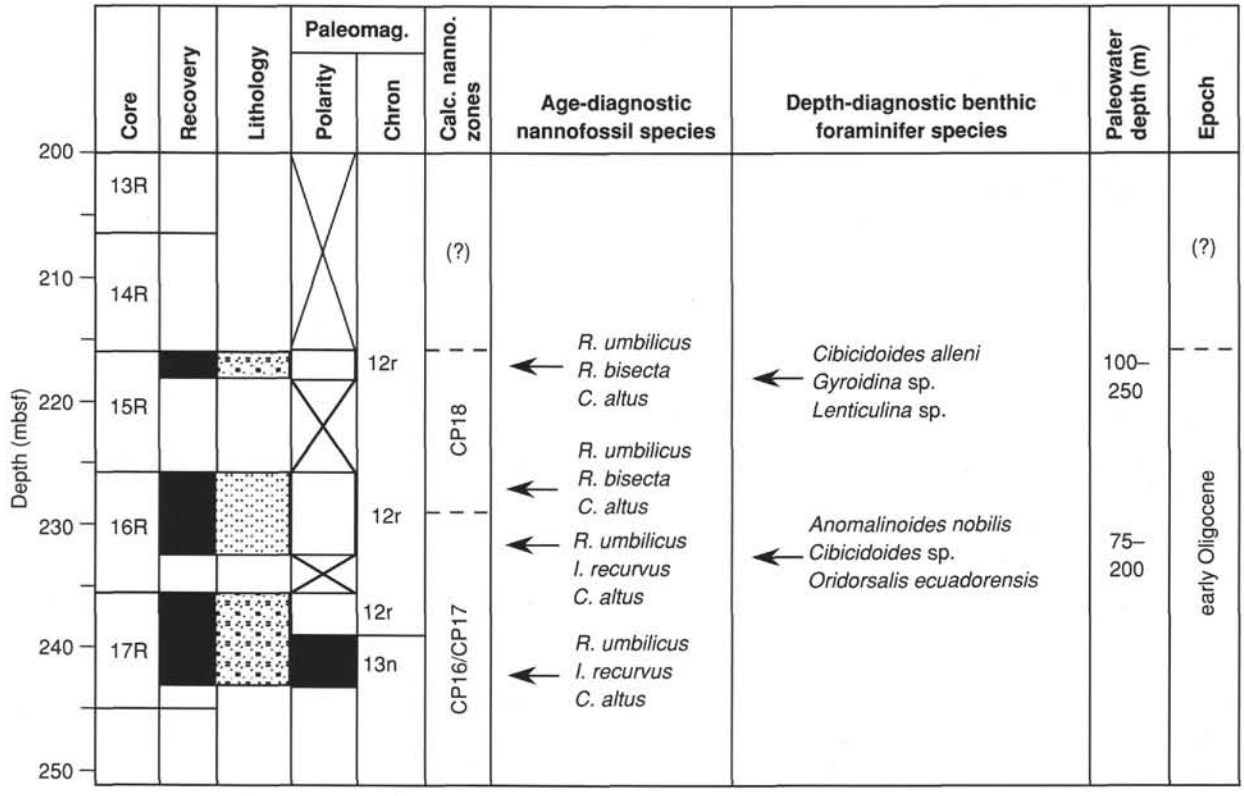

Figure 7. Biostratigraphic summary of Hole 914B. Paleowater depths inferred by benthic foraminiferal species also are shown.

Sample 152-914A-1H-1, 0–2 cm, contains common and well-preserved planktonic specimens of sinistrally coiled *N. pachyderma, G. glutinata, G. juvenilis*, and *T. quinqueloba*, along with rarer specimens of *N. dutertrei*. It also contains abundant and moderately preserved benthic specimens. *Eilohedra* sp., *Cibicides* spp., and *Cibicides refulgens* are common. *Cassidulina teretis* constitutes about 5% of the total benthic assemblage, compared to only 1% of *Elphidium excavatum*.

The planktonic foraminiferal assemblage in Sample 152-914A-1H-1, 32–35 cm, consists of common to a few moderately preserved specimens of sinistrally coiled *N. pachyderma, G. bulloides, T. quinqueloba, G. juvenilis*, and *G. glutinata*, rare *N. dutertrei* and extremely rare specimens of *Tenuitella anfracta, Hastigerinopsis riedeli*, and *Gallitellia vivans*. The benthic foraminiferal assemblage consists of abundant and moderately preserved specimens of *Cibicides* spp., *Cassidulina teretis*, which constitutes more than 20% of the benthic assemblage, *Cibicides refulgens*, and *Cibicides lobatulus*, along with rarer specimens of *Elphidium excavatum* (1%).

Sample 152-914A-1H-1, 95–97 cm, contains only rare, moderately preserved sinistrally coiled specimens of *N. pachyderma,* along with rarer *G. juvenilis* and *G. glutinata*. However, the sample contains common and moderately preserved benthic specimens. Buliminella *elegantissima* is abundant and *Cassidulina norvangi* is common. *Cassidulina teretis* constitutes only 5% and *Elphidium excavatum* 1% of the benthic assemblage, respectively.

In Sample 152-914A-1H-2, 83–85 cm, the planktonic foraminiferal assemblage consists only of rare, moderately preserved sinistrally coiled specimens of *N. pachyderma*. The benthic fauna comprise only few and moderately preserved specimens, consisting predominantly of *Elphidium excavatum*, which contributes 15% of the total benthic fauna. Also identified are *Cibicides* spp., *Cassidulina norvangi*, *Stainforthia* sp., and *Cassidulina teretis*, which constitutes 10% of the assemblage.

Sample 152-914A-1H-1, 95–97 cm, contains only rare, moderately preserved sinistrally coiled specimens of *N. pachyderma* and a few moderately preserved benthic foraminifers. The benthic assemblage is dominated by *Elphidium excavatum, Cassidulina norvangi, Nonionellina labradorica*, and *Cassidulina teretis*. *Cassidulina teretis* and *Elphidium excavatum* contribute 10% and 15% of the benthic fauna, respectively.

Table 5. Composition of calcareous sandstone (interval 152-914B-13R-CC, 10–14 cm) based on a count of 500 points.

Composition	Percentage (%)	Remarks
Quartz	38	Single grains.
Feldspar	7	
Calcite	38	Cement matrix of rock.
Amphibole	5	Mostly plutonic.
Opaque minerals	1	
Epidote	1	
Clinopyroxene	tr	
Chlorite	tr	
Rock fragments		
Quartzite	6	
Gneiss	1	
Granitic rocks	1	
Metapelite	1	
Unknowns	1	
Volcanic rocks	tr	
Schist	tr	
Ultramafic (?)	tr	

Note: Trace amounts (tr) are less than 1% of points counted.

In Sample 152-914A-1H-2, 132–135 cm, the planktonic foraminiferal assemblage consists only of rare, moderately preserved, sinistrally coiled specimens of *N. pachyderma* (Fig. 9) and a few, moderately preserved benthic foraminiferal specimens. *Cassidulina norvangi*, *Cassidulina teretis*, and *Elphidium excavatum* are relatively common, with the latter two species constituting 10% and 15% of the benthic assemblage, respectively (Table 6).

Aksu et al. (1989) suggested that during the North Atlantic glacial stages, the very low-diversity planktonic foraminiferal assemblages

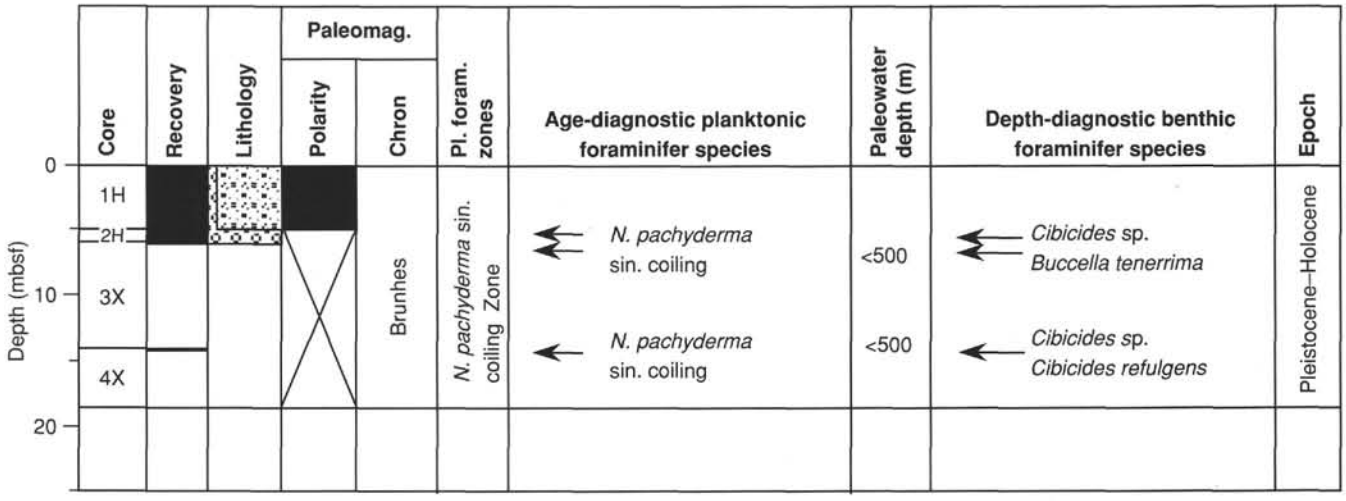

Figure 8. Biostratigraphic summary of Hole 914A. Paleowater depths inferred by benthic foraminiferal species also are shown.

Table 6. List of selected species of benthic foraminifers from Sections 152-914A-1H-1 and -2.

Core, section, interval (cm)	*Angulogerina angulosa*	*Anomalina grablata*	*Anomalina* sp.	*Buccella tenerrima*	*Buliminella elegantissima*	*Cassidulina norvangi*	*Cassidulina teretis*	*Cibicides lobatulus*	*Cibicides refulgens*	*Cibicides* spp.	*Eilohedra* sp.	*Elphidium excavatum*	*Elphidium subarcticum*	*Elphidium* spp.	*Fissurina marginata*	*Fissurina orbignyana*	*Gyroidina* sp.	*Islandiella norcrossi*	*Islandiella* sp.	*Nonionellina labradorica*	*Pullenia bulloides*	*Stainforthia* sp.	*Triloculina tricarinata*	Totals
152-714-1H-1, 0–2	4	2	1	0	0	13	12	17	38	43	49	2	2	10	2	1	1	0	5	3	3	0	0	263
152-714-1H-1, 32–35	2	3	2	3	0	6	47	24	32	54	2	2	3	0	1	0	0	0	0	1	4	1	0	207
152-714-1H-1, 95–97	0	0	3	6	62	26	13	1	1	15	2	2	2	2	0	0	0	0	1	0	0	3	0	192
152-714-1H-2, 83–85	2	2	1	6	6	30	20	3	5	32	2	37	1	4	0	1	0	0	0	14	1	21	0	222
152-714-1H-2, 96–98	1	4	0	3	7	36	19	5	5	8	4	40	0	0	2	0	1	4	4	24	0	16	2	211
152-714-1H-2, 135–137	1	3	0	6	2	37	22	2	8	11	6	50	0	1	0	0	0	3	5	15	0	7	1	203

Note: Total numbers of counted benthic specimens in each sample are reported in last column.

were dominated by sinistrally coiled specimens of *N. pachyderma*, with various percentages of *T. quinqueloba, G. bulloides*, and dextrally coiled specimens of *N. pachyderma*. Rare specimens of *N. dutertrei* and globorotaliids also may be present. Interglacial intervals, on the other hand, are characterized by higher species diversity and a fauna dominated by dextrally coiled specimens of *N. pachyderma, G. bulloides*, and *G. inflata*, with lower percentages of *N. dutertrei*, globorotaliids, and *T. truncatulinoides*.

Moreover, glacial intervals on the Rockall Plateau in the North Atlantic are characterized by the occurrence of the benthic species *Cassidulina teretis* (Murray, 1984). In ODP Hole 644A (water depth, 1226.3 m), on the Vøring Plateau of the North Atlantic, glacial intervals are dominated by the same species (synonym of *Cassidulina laevigata*), with abundant *Elphidium excavatum*, which has been interpreted as a reworked shallow-water species (Osterman and Qvale, 1985). Because the water depth in Hole 914A is only 533 m and because no difference in the degree of preservation is seen between *Elphidium excavatum* and the other Quaternary species, this species may be considered to be in situ and may indicate a shallow-water glacial environment.

Both the planktonic and benthic assemblages of Sample 152-914A-1H-1, 0–2 cm, suggest a post-glacial environment.

The benthic assemblage in Sample 152-914A-1H-1, 32–35 cm, suggests the presence of the transition to a glacial environment within the upper 30 cm of sediments. However, the planktonic foraminiferal assemblage does not appear to be consistent with this interpretation, because of the presence of very few specimens of *T. anfracta* and *H. riedeli*, which Kennett and Srinivasan (1983) suggested as a tropical species. However, their presence, previously documented in this area by Poore (1979), may result from an influx of relatively warmer surface water from the Central North Atlantic toward the Labrador Sea during the early to middle stages of major ice-growth phases of the late Quaternary (Ruddimann et al., 1980; Aksu et al., 1989).

A transition to an interglacial environment, occurring at a depth of about 95 cm, is also suggested by benthic assemblages that show low abundances of *Cassidulina teretis* and *Elphidium excavatum*.

A glacial environment has been tentatively inferred from benthic assemblages that consist of common *Elphidium excavatum* and *Cassidulina teretis* and from a planktonic assemblage that consists of the cold-water planktonic species *N. pachyderma* in three samples from Section 152-914A-1H-2.

PALEOMAGNETISM

Paleomagnetic data were obtained from Holes 914A and 914B. All remanence data from Hole 914A are from WCC studies on the archive-half sections of Core 152-914A-1H (although drilling continued to Core 152-914A-4H, minimal recovery, combined with excessive drilling disturbance, rendered studies of this interval meaningless, and the cores were not measured). Initial natural remanent magnetization (NRM) intensities of Core 152-914A-1H typically were 100 to 500 mA/m. Demagnetization to 30 mT reduced the intensities to between 20% and 30% of the initial values. Core 152-914A-1H is of consistent normal polarity and has a characteristic mean inclination angle of

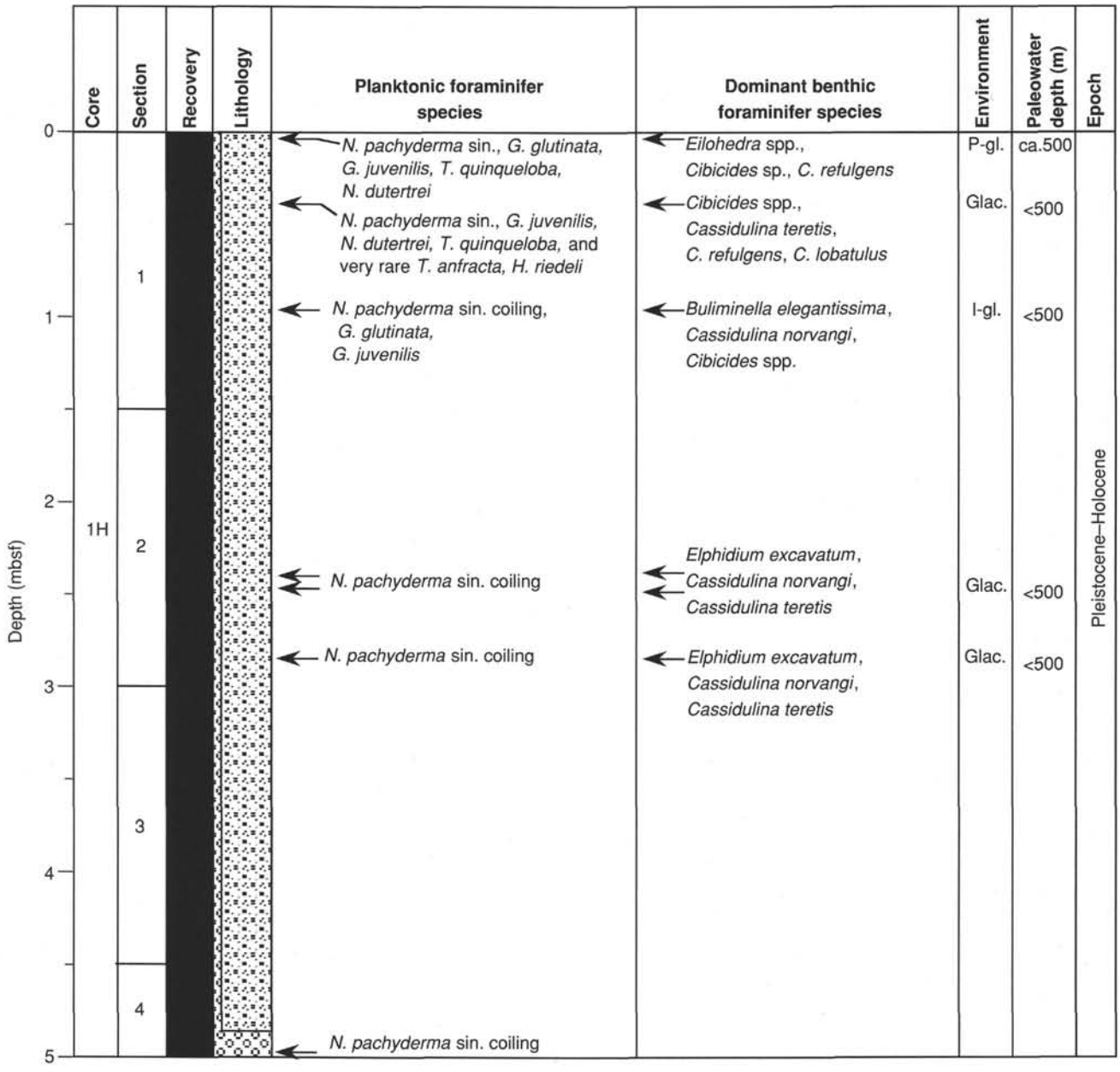

Figure 9. Biostratigraphic summary of Core 152-914A-1H. Planktonic and benthic foraminiferal assemblages have been used to identify tentatively glacial and post-glacial environments. Paleowater depths inferred by benthic foraminiferal species also are shown; P-gl. = post-glacial; Glac. = glacial; I-gl. = interglacial.

about 70° (Fig. 10), except where the remanence has been disturbed, either from the presence in the core of centimeter-scale dropstones or by the coring process itself. Foraminiferal data (see "Biostratigraphy" section, this chapter) indicate a Quaternary age for these sediments. The normal polarity remanence probably represents a record of part of the Brunhes Chron.

In Hole 914B, paleomagnetic data were obtained from four cores (152-914B-13R, and -15R to -17R). Initial NRM intensities for material in each of these cores was typically 200 to 400 mA/m. Demagnetization to 30 mT reduced the intensities to between 1% and 5% of the initial values. Demagnetization by about 10 mT removed a steep downward-dipping remanence, which may possibly be a drilling-induced magnetization (e.g., Fig. 11). This component contributed about 90% of the initial NRM.

At interval 152-914B-13R-1, 3–18 cm, a thin calcareous sandstone recorded steep positive inclinations, indicating a normal polarity remanence. The two sections within Core 152-914B-15R include a number of core pieces having lengths of >5 cm. Remanence data from these pieces show consistent negative inclinations, indicating a reverse polarity magnetization (see Fig. 12). Core 152-914B-16R is of dominantly reverse polarity. The exception to this is seen at interval 152-914B-16R-3, 95–130 cm, where the 30-mT demagnetization revealed steep positive inclinations. This is in contrast to the pattern of behavior for the previous steps (up to 20 mT), where demagnetization indicated a systematic tracking toward negative inclinations. In Figure 12, this interval has been coded "?" to indicate anomalous behavior. The same phenomenon occurred between Sections 152-914B-17R-2, 70 cm, and -17R-3, 40 cm. The upper part of Core 152-914B-17R (down to Section 152-914B-17R-3, 75 cm) is of dominantly reverse polarity. Below this level, steep positive inclinations were recorded, indicating a normal polarity remanence.

Biostratigraphic data (see "Biostratigraphy" section, this chapter) allowed us to correlate these magnetozones to the geomagnetic polarity time scale. The reverse polarity remanence associated with Cores

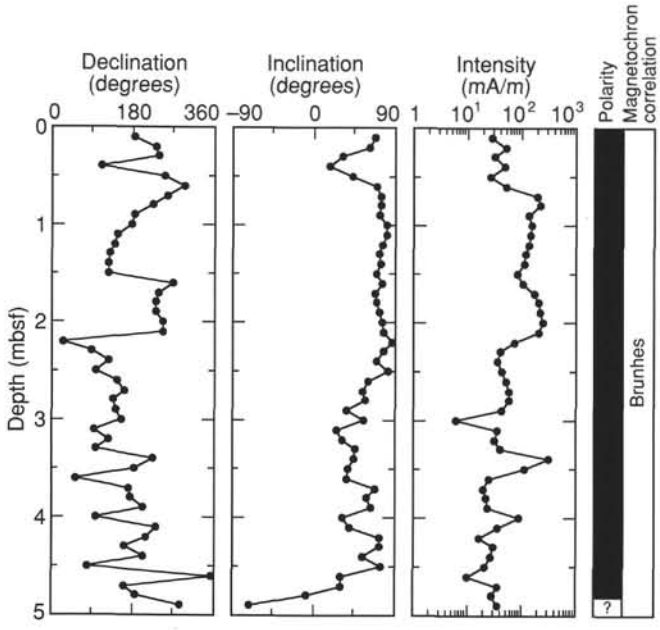

Figure 10. Remanence data from Core 152-914A-1H (0–5 mbsf) following the 30-mT demagnetization step. Shown are declination, inclination, and intensity data, as well as the inferred magnetic polarity of the core. As the cores were not oriented about a vertical axis, the declination data are defined with respect to the core's fiducial line. Biostratigraphic data suggest correlation of these normal polarity magnetized sediments with the Brunhes Chron.

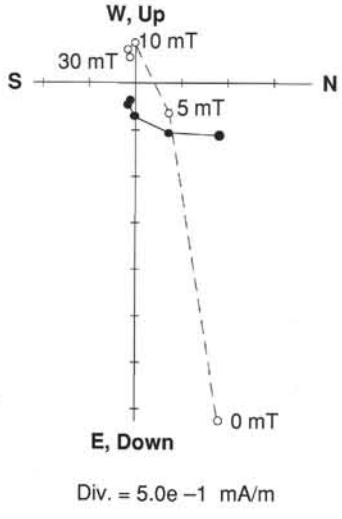

Figure 11. An example of the typical responses of material from Cores 152-914B-13R and -15R to -17R (at Section 152-914B-16R-1, 75 cm) to alternating field demagnetization. The paleomagnetic data have been plotted on pairs of orthogonal planes (Zijderveld, 1967). In these orthogonal plots, solid symbols represent points on the horizontal plane and open symbols points on the vertical plane. Demagnetization step values are shown adjacent to the vector plotted on the vertical plane. In this example, note the large contribution that the low-coercivity remanence (possibly drilling-induced) makes to the initial remanence. Demagnetization reveals a reverse polarity magnetization at 30 mT.

152-914B-15R and -16R probably represents a partial record of Chron C12r. Nannoplankton from this interval (the presence of *Reticulofenestra daviesii*, *R. umbilicus*, and *Chiasmolithus altus* and the absence of *Isthmolithus recurvus*) indicate an age of about 31 to 32 Ma. Polarity data from Core 152-914B-17R can be correlated with the geomagnetic polarity time scale in two ways (see Fig. 12), as the nannoplankton

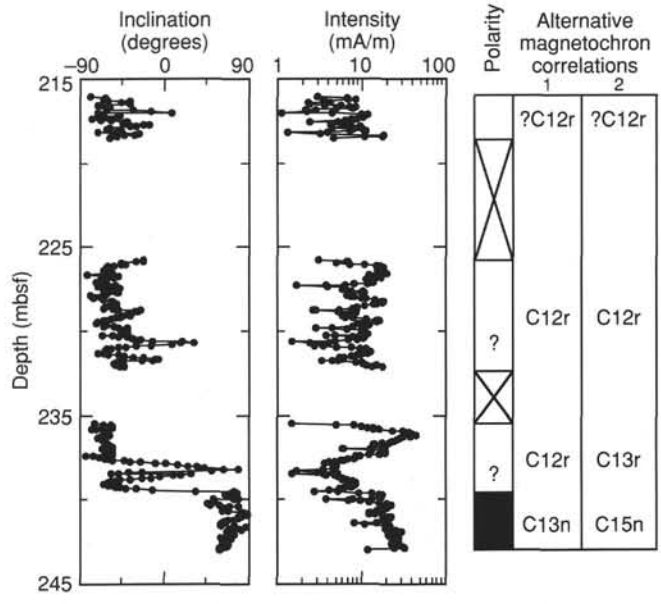

Figure 12. The 30-mT paleomagnetic data for Cores 152-914A-15R to -17R. Shown are the inclination and intensity data and the inferred polarity of the core. Although the biostratigraphic data permit alternative chron correlations for the magnetostratigraphy; (1) is considered the more likely (see text).

from this interval indicate an age range of between about 32 and 35 Ma (the presence of *Reticulofenestra daviesii*, *R. umbilicus*, *Chiasmolithus altus*, and *Isthmolithus recurvus*). Thus, the downhole transition from reverse to normal polarity at Section 152-914B-17R-3, 75 cm, may represent either the reversal between Chrons C12r and C13n or Chrons C13r and C15n. Because there is no biostratigraphic evidence for a significant discontinuity in Cores 152-914B-15A to -17A, the former interpretation is preferred.

SEDIMENTATION RATES

Only a few data points are available for constructing an age-vs.-depth diagram for Site 914 (Fig. 13). Nannofossils from Section 152-914B-8R-CC (158 mbsf) are younger than 1.7 Ma. This suggests a minimum sedimentation rate of 9.3 cm/k.y. for the interval from the seafloor to 158 mbsf. Sedimentation rates could not be calculated for the interval between 158 and 216 mbsf, as only a few pieces of gravel were recovered in this interval, for which biostratigraphy was not possible. Nannofossils older than about 31 Ma are present in Core 152-914B-15R. We assume that the top of this core at 216 mbsf is older than 31 Ma, and this provides another age-control point (Fig. 13). The third age-control point used is the top of C13n (33.0 Ma) at 239 mbsf. The interval between 216 and 239 mbsf thus has a minimum sedimentation rate of 1.2 cm/k.y. The last age-control point has been placed at the bottom of Core 152-914B-17R at 243 mbsf, which is younger than 33.5 Ma (the bottom of C13n). This results in a minimum sedimentation rate of 0.8 cm/k.y. for the interval between 239 and 243 mbsf.

ORGANIC GEOCHEMISTRY

As part of the shipboard safety and pollution monitoring program, concentrations of methane (C_1) and ethane (C_2) were monitored in every core, where sediment was recovered, using standard ODP headspace-sampling techniques. No significant amounts of gases were detected in the sediment column of Site 914.

Because of the limited core recovery, only 17 sediment samples for shipboard analysis could be collected from Core 152-914A-2H and Cores 152-914B-15R to -17R. Results are presented in Table 7 and Figure 14. The organic carbon content of the sediments remains

constantly low and ranges from 0.18 to 0.42 wt%. Total nitrogen values for these organic carbon-lean sediments are mostly near or below the detection limit of the shipboard NCS-analyzer. Sulfur content was below the detection limit in samples from Hole 914A. In samples from Hole 914B, total sulfur content varied between 0.17 and 0.53 wt%. The upper part of the sediment sequence shows calcium carbonate contents between 4 and 6 wt% (Hole 914A). In Hole 914B, however, values are distinctly lower and vary between 0 and 2 wt%.

A discussion of the results from the shipboard analyses from Site 914 is given in the "Organic Geochemistry" section, "Site 915" chapter (this volume).

INORGANIC GEOCHEMISTRY

Only four interstitial-water samples were obtained at Site 914. Methods are described in the "Inorganic Geochemistry" section of the "Explanatory Notes" chapter (this volume). The results obtained are presented in Table 8. The significance of the results is discussed in the "Inorganic Geochemistry" section, "Site 916" chapter (this volume). Sites 914, 915, and 916, which are in close proximity to each other and to the Greenland coast, form a complementary set of data.

PHYSICAL PROPERTIES

Introduction

Continuous downcore profiling of physical properties was limited by poor core recovery. Only two APC and no XCB cores were recovered. Much of the RCB core recovered was biscuited, which reduced the quality of the MST data and precluded strength testing. In most cases, sufficient core was not available to draw any detailed conclusions regarding the net downhole change in physical properties. However, sufficient data exist from individual units to gain some insight into their individual histories and, hence, to infer complete profile conditions.

Multisensor Track (MST)

With the exception of Core 152-914A-2H, all cores collected at Site 914 were processed through the MST. *P*-wave velocities were measured only for APC Core 152-914A-1H. Gamma-ray attenuation porosity evaluator (GRAPE) wet bulk density, magnetic susceptibility, and natural gamma data were collected for all cores. GRAPE-measured wet bulk density for RCB cores was corrected for drilling disturbance (reduced diameter), as detailed in the "Physical Properties" section, "Explanatory Notes" chapter (this volume).

The MST data suite of GRAPE wet bulk density, magnetic susceptibility, and natural gamma provides an excellent reference for evaluating changes in bulk sediment composition, sedimentary environment, depositional rate, and post-depositional compaction history. Magnetic susceptibility and natural gamma (total counts) measurements are particularly good indicators of bulk variation in sediment composition and, hence, changes in sediment source. MST data for Core 152-914A-1H highlight the lithologic changes in this core and provide clues to the depositional environment of the sediments.

Core 152-914A-1H consists of muds, interglacial sandy silts, and glacial diamictons of unknown age. Each of these units has a unique MST signature. The surficial Holocene muds exhibit a rapid increase in wet bulk density, magnetic susceptibility, and natural gamma with depth (Fig. 15). Interglacial sandy silts are relatively uniform in their signals. The glacial diamictons have high wet bulk densities, magnetic susceptibilities, and natural gamma counts. MST data for the diamictons are frequently spiked. This erratic signal may be the result of the increased clay content, and/or the inclusion of numerous clasts. The lithology of these clasts is highly variable, including abundant clasts of granitic composition, which are notorious for their erratic magnetic susceptibility and natural gamma signals.

Core 152-914B-15R consists of interbedded, indurated sands and silts. These sediments frequently were biscuited during drilling, which

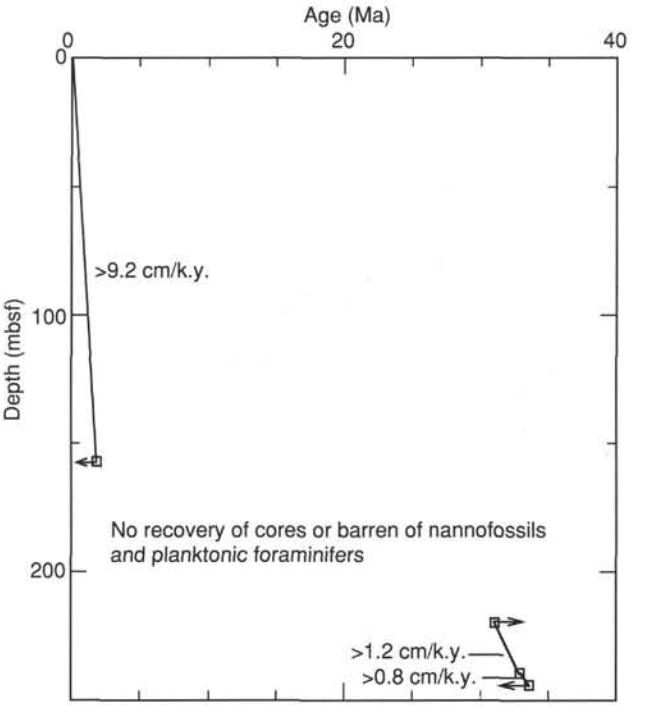

Figure 13. Diagram of age vs. depth for Site 914. Sedimentation rates for different stratigraphic intervals are shown.

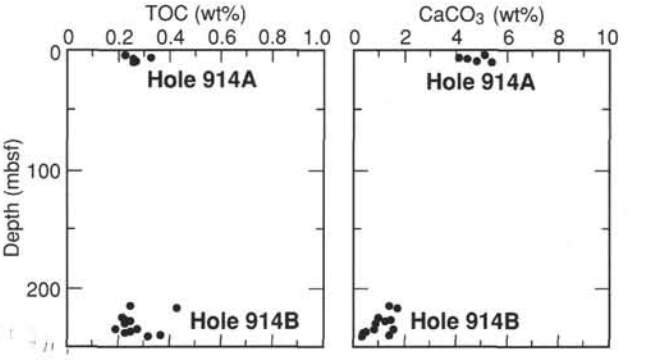

Figure 14. Results of total organic carbon (TOC) and calcium carbonate ($CaCO_3$) analyses vs. depth in sediments from Holes 914A and 914B.

resulted in erratic wet bulk densities. However, by carefully correlating core gaps with the MST records, we note that the sands are denser than adjacent silty bands. Wet bulk density of the sands within this interbedded unit decreases with depth, while the silt beds appear to remain constant. This suggests a greater sensitivity of sand beds to compactional dewatering.

Sediments recovered in Cores 152-914B-16R and -17R consist of volcanogenic silty sands that have a fairly uniform bulk density of 2.0 g/cm^3. These are grossly consistent in their natural gamma and magnetic susceptibility signals. The erratic GRAPE wet bulk density signal results from core gaps and drilling-induced damage. Small-scale, continuous variations most likely reflect the interbedded nature of the sediments. First-order variations, especially noticeable in the magnetic susceptibility signal, may indicate pulses of sedimentation and, hence, variation in sediment composition.

Index Properties

Wet bulk density, grain density, dry density, water content, porosity, and void ratio (see "Physical Properties" section, "Explanatory

Table 7. Summary of organic chemistry analyses at Holes 914A and 914B.

Core, section, interval (cm)	Depth (mbsf)	TC (wt%)	IC (wt%)	TOC (wt%)	$CaCO_3$ (wt%)	TN (wt%)	TS (wt%)
152-914A-							
2H-1, 16–17	5.16	0.83	0.6	0.22	5.08	0.00	0.04
2H-2, 72–74	6.73	0.81	0.5	0.32	4.08	0.00	0.05
2H-3, 28–29	7.79	0.78	0.5	0.25	4.41	0.00	0.00
2H-4, 143–144	10.44	0.83	0.6	0.26	4.75	0.00	0.05
2H-5, 19–20	10.70	0.89	0.6	0.25	5.33	0.00	0.06
152-914B-							
15R-1, 111–113	217.21	0.40	0.2	0.24	1.33	0.00	0.17
15R-2, 91–93	218.43	0.62	0.2	0.42	1.67	0.02	0.37
16R-1, 127–128	227.07	0.32	0.1	0.21	0.92	0.01	0.22
16R-2, 124–126	228.54	0.39	0.2	0.22	1.42	0.00	0.20
16R-3, 128–130	230.08	0.38	0.1	0.24	1.17	0.02	0.22
16R-4, 125–126	231.55	0.32	0.1	0.22	0.83	0.00	0.21
17R-1, 85–86	236.35	0.45	0.2	0.27	1.50	0.02	0.40
17R-1, 131–132	236.81	0.27	0.1	0.18	0.75	0.00	0.22
17R-2, 127–129	238.27	0.29	0.1	0.24	0.42	0.02	0.36
17R-3, 128–130	239.78	0.26	0.0	0.22	0.33	0.00	0.24
17R-4, 129–131	241.29	0.52	0.2	0.36	1.33	0.02	0.53
17R-5, 126–128	242.76	0.34	0.0	0.31	0.25	0.00	0.49

Note: TC = total carbon; IC = inorganic carbon; TOC = total organic carbon; $CaCO_3$ = calcium carbonate; TN = total nitrogen; TS = total sulfur.

Table 8. Chemical composition of interstitial waters at Site 914.

Core, section, interval (cm)	Depth (mbsf)	pH	Alkalinity (mM)	Salinity (g/kg)	Cl^- (mM)	Ca^{2+} (mM)	Mg^{2+} (mM)	Sr^{2+} (μM)	Li^+ (μM)	Na^+ (mM)	K^+ (mM)	SO_4^{2-} (mM)	NH_4^+ (μM)	H_4SiO_4 (μM)	B^{3+} (mM)	Mn^{2+} (μM)
Bottom water	0	8.10	2.35	34.9	557	10.4	54.0	87	27	480	10.40	29.0	0	50	0.42	0
152-914A-																
1H-2, 140–150	3	7.89	4.24	34.2	543	12.1	48.3	90	18	483	11.50	27.8	177	550	0.47	20.8
2H-3, 0–10	10	8.15	2.57	34.2	552	13.9	43.8	97	19	487	10.50	29.2	317	380	0.22	
152-914B-																
15R-1, 69–77	218	8.76	1.47	34.0	546	29.9	31.3	128	37	465	5.52	22.0	131	125	0.34	10.3
17R-4, 140–150	240	9.08	1.36	34.0	546	29.6	31.1	115	41	464	6.16	21.8	109	146	0.29	10.4

Notes" chapter, this volume) were determined for 30 discrete samples. These data are presented in Table 9 and illustrated in Figure 15.

Wet bulk density of the shallow sediments ranges from 1.70 to 1.80 g/cm^3 for very wet, surficial muds and well-sorted, sandy interglacial silts to 2.20 g/cm^3 for poorly sorted glacial diamictons. For all these sediments, the grain density remains approximately constant at 2.80 g/cm^3, while the water content diminishes rapidly. Given the relative consistency of the grain density values, the variations in bulk density must be controlled by fluctuations in water content. Water content is a sensitive indicator of sedimentary environmental conditions (e.g., rate of deposition), or post-depositional burial history.

For the deeper volcanogenic sands and silts, a subtle, but constant, increase is seen in water content and porosity with depth. The variations in grain density result from the fluctuation between silt and sand-dominated sediments. This is supported by the second-order changes in the magnetic susceptibility and natural gamma signals.

Velocimetry

The Hamilton Frame was used to measure compressional (*P*-wave) velocity for the stiff and indurated sediments of Cores 152-914B-15R to -17R. Velocities were measured in three directions: longitudinal (V_z), transverse (V_x), and transverse (V_y) (see "Physical Properties" section, "Explanatory Notes" chapter, this volume). Data are presented in Table 10 and illustrated in Figure 16. No digital sonic velocimeter (DSV) data were collected for soft sediments at Site 914 owing to equipment problems. Longitudinal velocities measured in Core 152-914B-15R decrease downcore from approximately 2.35 to 2.15 km/s. Longitudinal and transverse sonic velocities measured for Core 152-914B-16R range between 2.35 and 2.15 km/s, and 2.43 and 2.05 km/s, respectively, but show no principle pattern for sonic velocity. Interestingly, samples from these three cores tend to exhibit transverse sonic velocities that are slower than their longitudinal velocities.

Undrained Shear Strength

Soft sediments were recovered only in Cores 152-914A-1H and -2H. Core 152-914A-2H is problematic. Core penetration records state that the APC advanced only 1.0 m, yet 6.0 m of material was recovered (5.0–11.0 mbsf). Index property data (e.g., uniform water content, and bulk density) and shear strength (discussed below) support that this is not material that flowed in, but that an error must have occurred with the advance indicator.

Undrained shear strength data for Cores 152-914A-1H and -2H are presented in Table 11 and illustrated in Figure 17. Of interest is the extremely high strength (peak strength = 156 kPa) of the sediments between 6.00 and 6.50 mbsf. This material is a diamicton consisting of abundant granule- to pebble-sized gravel in a sandy clay matrix. The high gravel content from 8.00 to 10.00 mbsf precluded the insertion of the minivane into the sediment, and no tests were performed.

The validity of the strength of this material has been questioned, as the core (5.0–11.0 mbsf) had to be extruded from the core barrel using compressed air at a pressure of more than 4000 psi. This is thought not to have influenced the strength for three reasons: (1) material deeper than 7.0 mbsf exhibits a normal strength of 20 to 40 kPa, (2) the peak and residual strengths throughout the core show good separation, and (3) the water content of the material is consistent with the values in Core 152-914A-1H. Had a flowing in of plastic, followed by overstrengthening during extrusion, occurred, we would have expected that (1) the entire core was equally overstrengthened, (2) residual strengths were equal to the peak strengths, and (3) the water content of the material was different from the material recovered in Core 152-914A-1H.

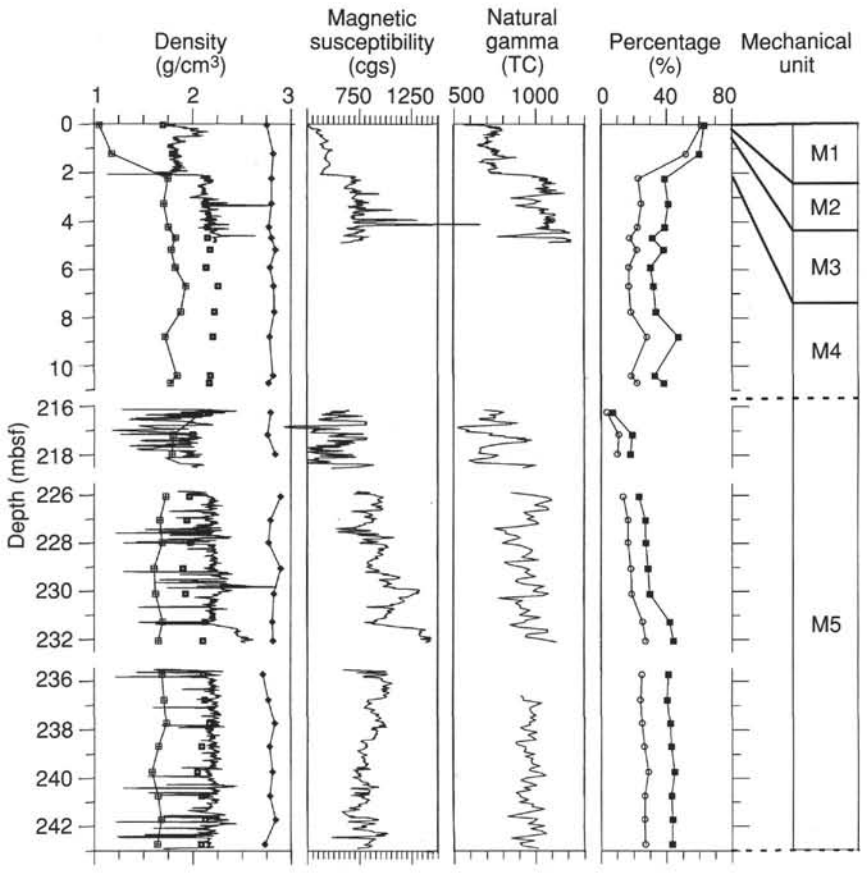

Figure 15. Composite plot of MST and discrete index property data for sediments recovered at Site 914: GRAPE wet bulk density (corrected for reduced diameter owing to RCB coring; see "Physical Properties" section, "Explanatory Notes" chapter, this volume), magnetic susceptibility, and natural gamma. Discrete measurements include wet bulk density (open squares), grain density (filled diamonds), dry density (hatched squares), water content (open circles), and porosity (filled squares).

Table 9. Index property data for Site 914.

Core, section, interval (cm)	Depth (mbsf)	Water content W_t (%)	Bulk density (g/cm³) MB	Grain density (g/cm³) MC	Dry density (g/cm³) MB	Porosity (%) MC	Void ratio MC
152-914A-							
1H-1, 5–7	0.05	61.34	1.70	2.75	1.05	63.11	1.65
1H-1, 124–126	1.24	51.89	1.80	2.82	1.18	59.92	1.43
1H-2, 75–77	2.25	22.66	2.15	2.80	1.75	38.77	0.62
1H-3, 28–30	3.28	24.68	2.13	2.80	1.71	41.17	0.68
1H-3, 124–126	4.24	22.62	2.15	2.78	1.75	38.76	0.61
1H-4, 19–21	4.69	17.58	2.15	2.80	1.83	31.40	0.48
2H-1, 18–20	5.18	21.87	2.18	2.84	1.79	38.13	0.61
2H-1, 93–95	5.93	16.98	2.14	2.79	1.83	30.26	0.46
2H-2, 70–72	6.71	16.95	2.26	2.82	1.93	31.96	0.47
2H-3, 25–27	7.76	18.32	2.22	2.83	1.88	33.60	0.51
2H-3, 129–131	8.80	28.04	2.21	2.78	1.72	47.15	0.76
2H-4, 140–142	10.41	18.22	2.18	2.82	1.84	32.77	0.50
2H-5, 22–24	10.73	22.07	2.16	2.77	1.77	38.23	0.60
152-914B-							
15R-1, 15–17	216.25	03.44	2.17	2.79	2.10	07.04	0.09
15R-1, 107–109	217.17	10.84	2.00	2.76	1.80	19.09	0.29
15R-2, 43–45	217.95	10.24	1.98	2.84	1.79	17.92	0.28
16R-1, 25–27	226.05	13.68	1.97	2.89	1.73	23.11	0.39
16R-1, 124–126	227.04	16.63	1.94	2.79	1.67	27.06	0.45
16R-2, 68–70	227.98	16.58	1.97	2.77	1.69	27.42	0.45
16R-3, 25–27	229.05	18.29	1.90	2.90	1.61	28.73	0.52
16R-3, 129–131	230.09	18.78	1.93	2.82	1.62	29.77	0.52
16R-4, 98–100	231.28	25.36	2.13	2.81	1.70	41.99	0.70
16R-5, 24–26	232.04	27.31	2.10	2.82	1.65	44.07	0.75
17R-1, 24–26	235.74	24.89	2.11	2.71	1.69	41.04	0.66
17R-1, 128–130	236.78	24.22	2.12	2.77	1.71	40.41	0.66
17R-2, 73–75	237.73	24.94	2.16	2.83	1.73	42.19	0.69
17R-3, 18–20	238.68	26.53	2.09	2.78	1.65	42.78	0.72
17R-3, 124–126	239.74	28.99	2.05	2.81	1.59	44.90	0.80
17R-4, 74–76	240.74	26.80	2.09	2.78	1.65	43.14	0.73
17R-5, 23–25	241.73	26.69	2.13	2.84	1.68	43.77	0.74
17R-5, 124–126	242.74	27.11	2.09	2.73	1.64	43.44	0.72

Note: Data were calculated according to Method B (MB) or Method C (MC) as defined in "Physical Properties" section, "Explanatory Notes" chapter (this volume).

Table 10. *P*-wave velocity measurements for Hole 914B.

Core, section, interval (cm)	Depth (mbsf)	Calculated velocity V_z (m/s)	V_x (m/s)	V_y (m/s)	Comments
152-914B-					
15R-1, 15–17	216.3	2876	3119	2947	
15R-1, 107–109	217.2	1464	1385		
15R-2, 43–45	218.0	2328	1365		
16R-1, 25–27	226.1	2356	2321	2345	
16R-1, 74–76	226.5	2296	2309	2273	
16R-1, 125–127	227.1	2273	2253	2307	
16R-2, 19–21	227.5	2321	2399		
16R-2, 80–82	228.1	1843	1842	1812	Very soft
16R-2, 121–123	228.5	2295	2309	2225	
16R-3, 19–21	229.0	2188	2152	2174	
16R-3, 89–91	229.7	2868	2956	2705	$CaCO_3$ cement
16R-3, 122–124	230.0	2265	2211	2249	
16R-4, 17–19	230.5	2268	2231	2219	
16R-4, 74–76	231.0	2237	2246	2216	
16R-4, 124–126	231.5	2217	2160	2156	
16R-5, 24–26	232.0	2156	2226	2208	
17R-1, 24–26	235.7	2238	2258	2256	
17R-1, 74–76	236.2	2248	2105	2174	
17R-1, 128–13	236.8	2136	2126	2084	
17R-2, 23–25	237.2	2349	2424	2425	
17R-2, 73–75	237.7	2211	2219	2236	
17R-2, 125–127	238.3	2226	2155	2163	Poor surface
17R-3, 18–20	238.7	2284	2295	2258	
17R-3, 72–74	239.2	2246	2216	2225	
17R-3, 123–125	239.7	2191	2208	2226	
17R-4, 22–24	240.2	2195	2140	2100	
17R-4, 74–76	240.7	2320	2261	2216	Well laminated
17R-4, 128–130	241.3	2209	2125	2117	Well laminated
17R-5, 24–26	241.7	2238	2048	2120	Well laminated
17R-5, 68–70	242.2	2157	2131	2102	
17R-5, 124–126	242.7	2188	2075	2062	Well laminated

Note: Longitudinal velocity V_z is perpendicular to core axis, transverse velocity V_x is parallel to bedding strike, transverse velocity V_y is perpendicular to bedding strike (see "Physical Properties" section, "Explanatory Notes" chapter, this volume).

Table 11. Undrained shear strengths measured at Sites 914, 915, and 917.

Core, section, interval (cm)	Depth (mbsf)	Undrained shear strength Peak (kPa)	Residual (kPa)	Remolded (kPa)
152-914A-				
1H-1, 41	0.41	22.8	12.5	5.9
1H-2, 44	1.94	20.5	4.0	5.4
1H-2, 110	2.60	29.4		
1H-3, 44	3.44	14.1	3.7	8.5
1H-3, 113	4.13	25.0	17.9	
1H-4, 31	4.81	26.2	23.4	11.8
2H-1, 23	5.23	20.1	3.6	30.4
2H-1, 89	5.89	151.0	115.3	
2H-2, 37	6.38	121.7	81.2	
2H-2, 113	7.14	23.0	11.1	
2H-5, 23	10.74	34.3	21.9	20.2
152-915A-				
1R-1, 41	0.41	13.4	3.7	16.1
1R-1, 136	1.36	48.8	21.5	
1R-2, 43	1.93	39.7	15.5	7.0
152-917A-				
1R-2, 49	1.99	9.0	3.2	13.0
1R-3, 62	3.62	11.0	7.2	15.4

Interbedded sands and silts recovered in Cores 152-914B-15R to -17R were too brittle to evaluate with the minivane. Testing was attempted with a handheld penetrometer, but in general, the more sandy materials have strengths in excess of the instrument maximum (4.5 kg/cm^2). The silts were tested similarly, but they tended to fail in a brittle manner, with the entire biscuit fracturing along bedding planes. Average forces required to fail the silts ranged from 2.0 to 3.5 kg/cm^2. The variation in failure strength for the silts is directly related to bed thickness, with the thicker beds requiring larger forces to produce failure.

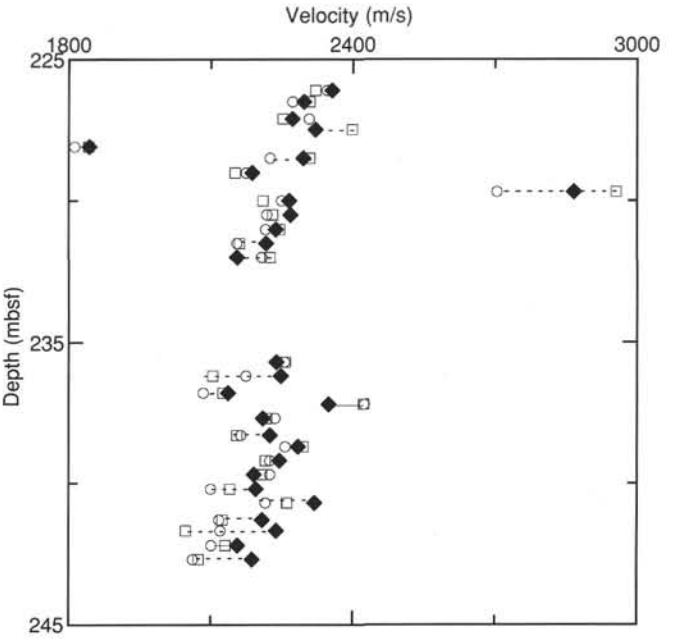

Figure 16. Discrete longitudinal and transverse sonic velocity data for sediments recovered in Hole 914B. Solid symbols = longitudinal velocity (V_z); open squares = transverse velocity (V_x); open circles = transverse velocity (V_y).

Resistivity and Thermal Conductivity

Resistivity was measured only for the soft, upper sediments in Cores 152-914A-1H and -2H. Values range from 0.52 to 4.60 Ωm. Resistivity data have been tabulated in Table 12 and are displayed in Figure 18. Insufficient material was available for minicore testing of the deeper recovered sections.

Full-space thermal conductivity measurements were performed for Cores 152-914A-1H, -914B-15R, and -17R. The deeper sediments were difficult to test, as they were frequently too stiff for the full-space method, but not sufficiently lithified for half-space testing. Thermal conductivity increases downcore from an average of 1.42 W/(m·K) in the soft sediments (lithologic Unit I), to 1.65 W/(m·K) for the deeper, semilithified, volcanogenic sands and silts (lithologic Unit II).

Summary

The sediments from Holes 914A and 914B may be divided into five distinct mechanical facies. Mechanical Units M1 through M4 correlate with lithologic Unit I, mechanical Unit M5 correlates with lithologic Unit II (see "Lithostratigraphy" section, this chapter). Mechanical Unit M1 (0–0.30 mbsf) comprises a thin sandy mud that correlates with the uppermost sediment of lithologic Subunit IA. Mechanical Unit M1 exhibits a rapid, linear change in its physical properties. Downcore within Unit M1, water content decreases from $W_t > 60\%$ to $W_t \approx 40\%$, while exhibiting increases in bulk density (from $\rho \approx 1.70$ to ≈ 2.10 g/cm^3), grain density (from $\rho_{grain} \approx 2.75$ to ≈ 2.80 g/cm^3), magnetic susceptibility (from 250 to 400 cgs), and natural gamma (from 500 to 800 TC). Given the rapid dewatering profile for Unit M1, we may infer that sedimentation rates for this surficial mud are very slow.

Mechanical Unit M2 (0.30–0.50 mbsf) consists of a thin silty sand with dropstones. The bulk density (average $\rho = 2.15$ g/cm^3) and natural gamma (NG = 800 TC) of Unit M2 are higher than sediments immediately above (Unit M1) or below (Unit M3). The pattern for all signals in Unit M2 is similar (though of lesser magnitude) to those of Unit M4 (described below). A marked decrease in bulk density sepa-

Table 12. Full-space thermal conductivity and electrical resistivity data for Sites 914, 915, and 916.

Core, section, interval (cm)	Depth (mbsf)	Thermal conductivity (W/[m•K])	Electrical resistivity (Ωm)
152-914A-			
1H-1, 25	0.25		0.806
1H-1, 70	0.70	1.256	
1H-2, 126	1.26		3.885
1H-2, 25	1.75		0.613
1H-2, 125	2.75		0.529
1H-2, 58	2.08	1.282	
1H-3, 25	3.25		0.734
1H-3, 60	3.60	1.781	
1H-3, 125	4.25		0.806
1H-4, 20	4.75	1.366	1.168
2H-1, 25	5.25		0.834
2H-2, 25	6.35		4.598
2H-2, 121	7.22		1.145
2H-3, 29	7.80		0.728
2H-3, 120	8.71		0.711
2H-4, 27	9.28		0.622
2H-4, 120	10.21		0.898
2H-5, 18	10.69		0.521
2H-6, 9	11.30		0.613
152-914B-			
15R-2, 2	216.12	1.978	
17R-1, 60	236.10	1.461	
17R-2, 60	237.60	1.427	
17R-4, 76	240.60	1.821	
17R-5, 65	242.15	1.576	
152-915A-			
1R-1, 30	0.30		0.771
1R-1, 60	0.60	1.247	
1R-1, 128	1.28		1.597
1R-2, 25	1.75		0.734
1R-2, 38	1.88	1.543	
18R-1, 49	149.10	1.351	
18R-2, 80	150.90	1.410	
18R-3, 122	152.80	1.308	
19R-1, 44	158.50	1.327	
19R-2, 59	160.20	1.769	
19R-4, 21	162.80	1.539	
21R-1, 89	168.80	1.424	
21R-2, 80	170.20	1.527	
21R-3, 54	171.40	0.818	
21R-4, 60	172.40	0.970	
21R-5, 33	173.20	1.434	
22R-1, 62	178.10	1.642	
22R-2, 60	179.60	1.861	
22R-3, 24	180.70	1.601	
152-916A-			
4R-2, 36	24.46		
4R-2, 40	24.50		
5R-1, 39	28.49	1.322	
13R-1, 86	79.60	1.078	
13R-2, 63	80.73	1.149	
13R-3, 63	82.23	1.591	
14R-1, 59	88.29	1.361	
14R-2, 73	89.93	1.396	
15R-1, 20	97.31	0.826	
15R-2, 61	97.64	0.855	
15R-3, 55	99.01	1.175	

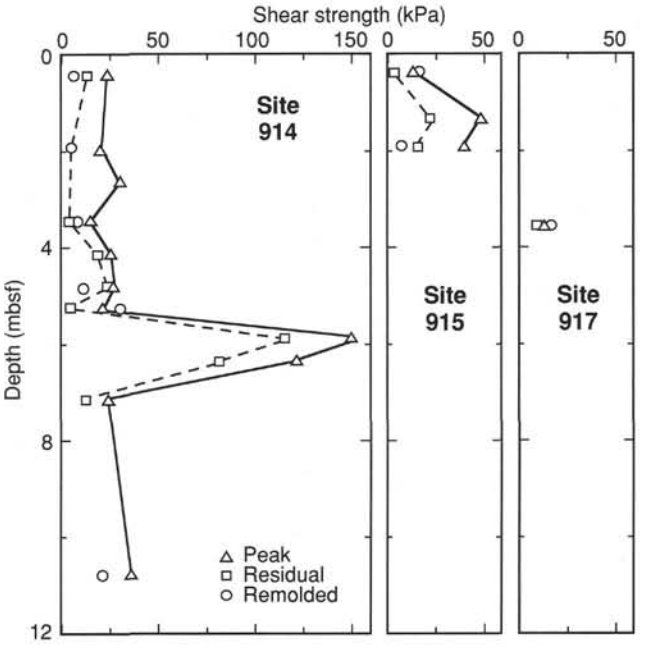

Figure 17. Undrained shear strengths for sediments recovered at Sites 914, 915, and 917.

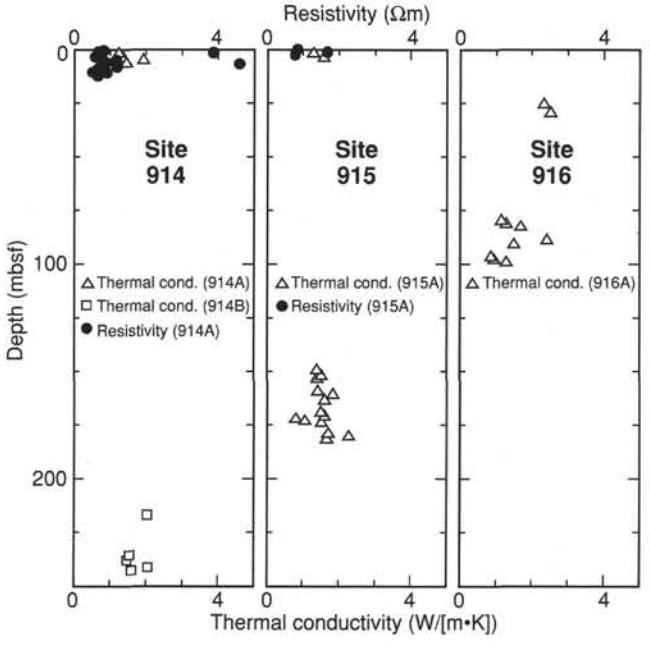

Figure 18. Resistivity and thermal conductivity data for sediments recovered at Sites 914, 915, and 916.

rates Unit M2 from the underlying Unit M3. Mechanical Unit M3 (0.50–2.10 mbsf) is characterized by its uniform bulk density (average $\rho = 1.85$ g/cm^3) and magnetic susceptibility (MS = 475 cgs). Only natural gamma shows any significant variation. This unit correlates with the interglacial sandy silts of lithologic Subunit IA (see "Lithostratigraphy" section, this chapter). Unit M4 is separated from the underlying glacial diamicton by sharp increases in bulk density, magnetic susceptibility, natural gamma, and shear strength, and by a corresponding sharp decrease in water content.

Sharp increases in bulk density, magnetic susceptibility, natural gamma, and shear strength, and a corresponding decrease in water content separate the sandy silts of Unit M3 from the underlying diamictons of mechanical Unit M4. Mechanical Unit M4 (2.10–11.00 mbsf) is made up of a poorly sorted mixture of lithic fragments in a fine-grained matrix. Discrete sampling defines the bulk density of the matrix as relatively uniform at $\rho = 2.10$ g/cm^3. The spiky nature of the GRAPE bulk density, magnetic susceptibility, and natural gamma reflect the numerous, lithologically diverse assemblage of clasts.

Mechanical Unit M5 comprises the deepest recovered sediments and correlates with lithologic Unit II. The interbedded volcanogenic sands and silts show considerable mechanical variation within the unit as a whole, but little variation between beds of similar lithology. The one major exception is the peculiar increase in porosity and water content with depth.

Ms 152IR-106

NOTE: For all sites drilled, core-description forms ("barrel sheets") can be found in Section 4, beginning on page 303. Forms containing smear-slide data can be found in Section 5, beginning on page 925. GRAPE, Index property, MAGSUS and Natural gamma-ray data are presented on CD-ROM (back pocket).